

Analysis of FETI methods for multiscale elliptic PDEs

C. Pechstein, R. Scheichl

RICAM-Report 2008-20

ANALYSIS OF FETI METHODS FOR MULTISCALE PDES

CLEMENS PECHSTEIN¹ AND ROBERT SCHEICHL²

ABSTRACT. In this paper we study a variant of the finite element tearing and interconnecting (FETI) method which is suitable for elliptic PDEs with highly heterogeneous (multiscale) coefficients $\alpha(x)$; in particular, coefficients with strong variation within subdomains and/or jumps that are not aligned with the subdomain interfaces. Using energy minimisation and cut-off arguments we can show rigorously that for an arbitrary (positive) coefficient function $\alpha \in L^\infty(\Omega)$ the condition number of the preconditioned FETI system can be bounded by $C(\alpha) (1 + \log(H/h))^2$ where H is the subdomain diameter and h is the mesh size, and where the function $C(\alpha)$ depends only on the coefficient variation in the vicinity of subdomain interfaces. In particular, if $\alpha|_{\Omega_i}$ varies only mildly in a layer $\Omega_{i,\eta}$ of width η near the boundary of each of the subdomains Ω_i , then $C(\alpha) = \mathcal{O}((H/\eta)^2)$, independent of the variation of α in the remainder $\Omega_i \setminus \Omega_{i,\eta}$ of each subdomain and independent of any jumps of α across subdomain interfaces. The quadratic dependency of $C(\alpha)$ on H/η can be relaxed to a linear dependency under stronger assumptions on the behaviour of α in the interior of the subdomains. Our theoretical findings are confirmed in numerical tests.

Keywords FETI · domain decomposition · iterative substructuring · finite element method · multiscale methods · preconditioning · varying coefficients

Mathematics Subject Classification (2000) 65F10, 65N22, 65N30, 65N55

1. INTRODUCTION

The advent of ever more powerful parallel computers and better imaging and tomography tools in recent years, has made it possible to carry out detailed simulations of biological, physical and engineering processes in complex geometries and with highly varying heterogeneous (often nonlinear) material parameters. Consequently, the development of efficient and robust parallel solvers for heterogeneous media has been a very active area of research, specifically in the setting of multiscale solvers, and in the domain decomposition and multi-grid communities [1, 2, 6, 7, 14, 15, 16, 17, 19, 31, 32, 33, 34, 38, 39]. In this paper we are particularly concerned with the convergence of a variant of the finite element tearing and interconnecting (FETI) method in the context of heterogeneous (multiscale) problems. As such the paper is a continuation of the work on Schwarz-type domain decomposition for multiscale PDEs in Graham, Lechner, and Scheichl [15], Graham and Scheichl [16, 17], as well as in Scheichl and Vainikko [35].

FETI methods are robust domain decomposition methods for solving finite element discretisations of partial differential equations (PDEs) with excellent parallel scalability properties. They belong to the class of dual iterative substructuring methods and were introduced

¹ Clemens Pechstein, SFB F013, Johannes Kepler University, Altenberger Str. 69, 4040 Linz, Austria, phone: (+43) 732 / 2468-9169, E-mail: clemens.pechstein@numa.uni-linz.ac.at

The first author has been supported by the Austrian Science Funds (FWF) under grant F1306.

² Robert Scheichl, Department of Mathematical Sciences, University of Bath, Bath BA2 7AY, United Kingdom, phone: (+44) 1225 / 386034, E-mail: r.scheichl@maths.bath.ac.uk .

by Farhat and Roux [13] in 1991. In contrast to primal iterative substructuring, the finite element subspaces are treated separately on each subdomain including its boundary. The global continuity across subdomain interfaces is enforced via Lagrange multipliers, which leads to a saddle point problem that can be solved iteratively via its dual problem. The dual problem is symmetric positive semi-definite and can be solved efficiently by a preconditioned conjugate gradient (PCG) subspace iteration. The key to a robust method is a special choice for the preconditioner. The basic ingredients for this preconditioner are efficient local Dirichlet- and Neumann-solvers for the subdomains and carefully chosen scalings.

The classical FETI methods and the more recently developed dual-primal FETI (FETI-DP) methods [12], as well as balancing domain decomposition by constraints (BDDC) [8, 24] are well established in the field of robust parallel solvers for large-scale finite element systems. Here we refer the reader to the monograph [37] by Toselli and Widlund, as well as to the recent articles [18, 19, 23, 25, 30]. The great success of FETI, FETI-DP, and BDDC methods is certainly due to their wide applicability, moderate complexity, excellent parallel scalability, and due to their robustness. The latter properties are not only observed numerically, but they have been established rigorously. In their pioneering work [26], Mandel and Tezaur gave the first convergence proof for one-level FETI methods with non-redundant Lagrange multipliers for two-dimensional elliptic problems with homogeneous coefficients. They showed that the spectral condition number of the corresponding preconditioned system is bounded by

$$(1.1) \quad C(1 + \log(H/h))^\beta,$$

with $\beta = 3$ (or $\beta = 2$ under certain assumptions on the subdomain partition). Here, as usual, H and h denote the subdomain diameter and the mesh width, respectively, and C is a constant independent of H and h . A better poly-logarithmic dependency, i. e., $\beta = 2$, was established by Klawonn and Widlund in [21]. They also extended the FETI method and its analysis to 3D problems with heterogeneous coefficients and to the case of redundant Lagrange multipliers (which are usually used in parallel implementations). Furthermore, assuming that the coefficients of the PDE are constant on each subdomain, they showed that the constant C in (1.1) is independent of possible jumps in the coefficients across subdomain interfaces when a special scaling of the preconditioner is applied. The same kind of bound for the preconditioned systems, i. e., (1.1) with $\beta = 2$, was also shown to hold true for FETI-DP methods and for the related balancing Neumann-Neumann and BDDC methods [21, 22, 25, 27]. The sharpness of the bound (with $\beta = 2$) was established by Brenner in [4], see also Brenner and He [5]. A comprehensive analysis of FETI and FETI-DP methods is contained in the monograph [37] by Toselli and Widlund.

All these analyses assume that the coefficients are piecewise constant with respect to the subdomain partitioning. The main focus of the present work is the analysis of FETI methods for highly heterogeneous multiscale problems, i. e., in the case of coefficient jumps that are not aligned with the subdomain interfaces and/or vary strongly within a subdomain. It has already been observed numerically by several authors (see [19, 23, 31, 32]) that a simple generalisation of the scaling employed by Klawonn and Widlund in [21] leads to robustness of the FETI method even in this case. However, a theoretical justification for this kind of robustness is still lacking. In the following, we restrict ourselves to the model elliptic problem

$$(1.2) \quad -\nabla \cdot (\alpha \nabla u) = f,$$

in a bounded polygonal or polyhedral domain $\Omega \subset \mathbb{R}^d$, $d = 2$ or 3 , subject to suitable boundary conditions on the boundary $\partial\Omega$. The coefficient $\alpha(x)$ may vary over many orders of magnitude in an unstructured way on Ω . We are able to show that the above bound (1.1) also

holds in this case with $\beta = 2$, but with $C = C(\alpha)$ in general. The key finding of the present work, however, is that this dependency of the condition number of the preconditioned system on the coefficient variation is restricted to the variation of α in the vicinity of subdomain interfaces (within each subdomain). More precisely, if $\Omega_{i,\eta}$ denotes the boundary layer of width η of any of the subdomains Ω_i , and if (locally) $\alpha(x) \leq C_\eta \alpha(y)$ for all $x, y \in \Omega_{i,\eta}$, then $C(\alpha) = C_\eta (H/\eta)^2$, independent of the variation of α in the remainder $\Omega_i \setminus \Omega_{i,\eta}$ of each subdomain and independent of any jumps of α across subdomain interfaces. Thus, we are able to recover the existing theory for the case where α is piecewise constant with respect to the subdomain partitioning, but we see that FETI methods can be robust even when α varies strongly within a subdomain or when coefficient jumps are not resolved by the subdomain partitioning. The quadratic dependency of $C(\alpha)$ on H/η can be relaxed to a linear dependency under stronger assumptions on the behaviour of α in the interior of the subdomains. Our theoretical results are confirmed in a series of numerical tests.

However, our numerical experiments also show that our bound is not always sharp when the coefficient varies strongly near subdomain interfaces. In practice FETI methods often seem to be robust even in this case, in particular when the variation along the interface is smooth or when the coefficient jumps only in a few places. The analysis in this case is much harder and will be the focus of future investigations. For the theoretical statements in this paper, we have assumed for convenience that α in (1.2) is a positive scalar function in $L^\infty(\Omega)$. However, the analysis applies in an analogous way when $\alpha(x)$ is replaced by a symmetric positive definite matrix $\mathcal{A}(x)$, with spectrum lying in the range $[c^{-1}\alpha(x), c\alpha(x)]$ where c is moderate in size, and where the scalar function $\alpha(x)$ has the properties which we assume below. The case when c is very large (i. e., the anisotropic case) presents additional difficulties and should be the subject of future analysis. We concentrate here only on the analysis of one-level FETI, but all the results can be easily extended to the FETI-DP and BDDC methods (see upcoming paper for details).

The paper is organised as follows. We start with some preliminaries in Section 2. In Section 3 we describe our generalisation of the one-level FETI method to multiscale PDEs. This section ends with the statement of our key result. The proof of the key result is postponed to Section 4. We conclude the paper with a series of numerical experiments in Section 5 and an appendix containing some technical proofs that we need for our key result.

2. PRELIMINARIES

In this section, we introduce some notation concerning in particular geometry, our elliptic model problem, and finite elements.

Throughout this work, $a \lesssim b$ means that some (generic) constant $C > 0$ exists with $a \leq Cb$. In particular, C will never depend on any mesh parameters h_i , (sub)domain diameters H_i , the coefficient $\alpha(\cdot)$, or the width parameters η_i introduced later in this paper, but only on shapes of (sub)domains or elements. Additionally, $a \simeq b$ stands for $a \lesssim b$ and $b \lesssim a$.

2.1. Model problem and subdomain partition. We consider an open connected domain $\Omega \subset \mathbb{R}^d$, $d = 2$ or 3 with boundary $\partial\Omega$. Defining the space $H_0^1(\Omega) := \{v \in H^1(\Omega) : v|_{\partial\Omega} = 0\}$, the variational formulation of our model problem (1.2) reads: Find $u \in H_0^1(\Omega)$ such that

$$(2.1) \quad \int_{\Omega} \alpha(x) \nabla u(x) \cdot \nabla v(x) dx = \int_{\Omega} f(x) v(x) dx \quad \forall v \in H_0^1(\Omega),$$

with $f \in L^2(\Omega)$.

We decompose the computational domain Ω into finitely many non-overlapping subdomains Ω_i , $i = 1, \dots, N$ and denote the subdomain boundaries by $\partial\Omega_i$. The subdomain interfaces Γ_{ij} are defined by $\Gamma_{ij} = (\partial\Omega_i \cap \partial\Omega_j) \setminus \partial\Omega$. Furthermore we define the *interface* Γ by

$$(2.2) \quad \Gamma := \bigcup_{i \neq j} \Gamma_{ij},$$

and the subdomain diameters by $H_i := \text{diam } \Omega_i$.

In the following we need some regularity assumptions on the subdomain partition.

Definition 2.1 (regular domain). For $d = 2$ (or 3), let $D \subset \mathbb{R}^d$ be a bounded contractible domain with a simply-connected Lipschitz boundary. D is called a *regular domain*, if it can be decomposed into a conforming coarse mesh of shape-regular triangles (tetrahedra). Whenever considering a family of regular domains, such as partitions into subdomains, we implicitly assume that the number of simplices forming an individual subdomain is uniformly bounded.

Definition 2.2 (shape parameter). We define the *shape parameter* of a regular domain D by $\rho(D) := \min_{1 \leq i \leq s} \rho(T_i)$, where $\{T_i\}_{1 \leq i \leq s}$ are the simplices according to Definition 2.1.

Definition 2.3 (shape-regular partition). Let D be an open domain in \mathbb{R}^2 or \mathbb{R}^3 . A family of partitions of D into regular subdomains $\{D_i\}_{i=1, \dots, N}$, such that $\bar{D} = \bigcup_{i=1}^N \bar{D}_i$, is called *shape-regular*, if

$$\rho(D_i) \simeq \text{diam } D_i, \quad \text{and} \quad \bar{D}_i \cap \bar{D}_j \neq \emptyset \implies \text{diam } D_i \simeq \text{diam } D_j \quad \forall i, j = 1, \dots, N.$$

Assumption A1. The subdomains $\{\Omega_i\}$ form a non-overlapping shape-regular partition of Ω , and the underlying coarse mesh (cf. Definition 2.1) is conforming.

Definition 2.4 (faces, edges, vertices). The interface Γ is the union of

- subdomain *faces*, regarded as open sets, that are shared by two subdomains,
- subdomain *edges*, also regarded as open sets, that are shared by more than two subdomains,
- *vertices*, which are endpoints of edges.

We denote by

- \mathcal{V}_i the set of vertices of Ω_i ,
- \mathcal{E}_i the set of edges of Ω_i ,
- \mathcal{F}_i the set of faces of Ω_i ,

and set $\mathcal{V} := \bigcup_{i=1}^N \mathcal{V}_i$, and $\mathcal{E} := \bigcup_{i=1}^N \mathcal{E}_i$, as well as $\mathcal{F} := \bigcup_{i=1}^N \mathcal{F}_i$. For convenience we introduce $\mathcal{X}_i := \mathcal{V}_i \cup \mathcal{E}_i \cup \mathcal{F}_i$.

For simplicity we have assumed Dirichlet boundary conditions on the whole of $\partial\Omega$. The case of Neumann boundary conditions on a part of $\partial\Omega$ is treated in detail in [37] and poses no principal difficulties. Nevertheless, we need a technical assumption on the partition and the Dirichlet boundary for the one-level FETI methods presented in this work, cf. [21, Assumption 1].

Assumption A2. We assume that in three dimensions, $\partial\Omega_i \cap \partial\Omega$ is either empty or contains at least an edge of the subdomain Ω_i .

Remark 2.5. Our assumptions on the regularity of the subdomains are typical for iterative substructuring methods, cf. [37, Assumption 4.3]. See, however, the recent works on domain decomposition methods for irregular subdomains in two dimensions, [9, 20].

2.2. Discretisation. For each subdomain Ω_i , we consider a quasi-uniform triangulation \mathcal{T}_i by triangles or tetrahedra with the mesh parameter h_i . The resulting global mesh is assumed to be conforming, i. e., the subdomain meshes match on the subdomain interfaces. This means, that for two neighbouring subdomains Ω_i and Ω_j the mesh sizes are comparable, $h_i \simeq h_j$. The nodes of the mesh on the local boundaries $\partial\Omega_i$ are denoted by $\partial\Omega_i^h$, and similarly we define Γ^h and Γ_{ij}^h to be the set of nodes on the interface Γ and on the subdomain interfaces Γ_{ij} , respectively. A typical node will be denoted by x^h . For the discretisation of (2.1) we use continuous piecewise linear finite elements. We denote by $V^h(\Omega)$, $V^h(\Omega_i)$ and $V^h(\partial\Omega_i)$ the spaces of continuous functions on the domain Ω , the subdomains Ω_i and the local boundaries $\partial\Omega_i$, respectively, which are piecewise linear on the elements of the mesh and fulfil the essential boundary conditions on $\partial\Omega$. For the sake of simplicity, we make no difference between functions on discrete spaces and their vector representations with respect to the standard nodal basis, as well as between operators and their matrix representations with respect to the same basis. Similarly, we identify any discrete space X with its dual space X^* .

On the subdomain Ω_i , we can assemble the local finite element stiffness matrix K_i and group it with respect to the unknowns on the interface (subscript Γ) and the interior (subscript I),

$$(2.3) \quad K_i = \begin{pmatrix} K_{i,\Gamma\Gamma} & K_{i,\Gamma I} \\ K_{i,I\Gamma} & K_{i,II} \end{pmatrix}.$$

Note that on the subdomains Ω_i that have a contribution from the Dirichlet boundary $\partial\Omega$, the stiffness matrix K_i (which corresponds to the local mixed boundary value problem) is invertible. Conversely, if Ω_i does not touch $\partial\Omega$, the stiffness matrix K_i corresponds to the pure Neumann problem and is therefore singular. If $\partial\Omega_i \cap \partial\Omega = \emptyset$, we call Ω_i a *floating subdomain*; the remaining subdomains are the *non-floating subdomains*. In the floating case (since we consider the operator $-\nabla \cdot (\alpha \nabla)$) the kernel of K_i consists of the constant functions on Ω_i , and so it has dimension 1.

The Galerkin projection of (2.1) onto the space $V^h(\Omega)$ (which includes the essential boundary conditions) leads to the following linear system. Find $\tilde{u} \in V^h(\Omega)$ such that

$$(2.4) \quad \tilde{K} \tilde{u} = \tilde{f},$$

where \tilde{K} is the global FE stiffness matrix (which can be obtained by assembling the local stiffness matrices K_i) and \tilde{f} is the load vector corresponding to the right hand side f in (2.1). FETI methods are special domain decomposition methods to solve system (2.4) in parallel. The common idea of these methods is to decouple the system subdomain-wise and to enforce the continuity of \tilde{u} by Lagrange multipliers λ . There exist various strategies to eliminate the primal variables, i. e., the decoupled degrees of freedom of \tilde{u} , and to design parallel preconditioners for the dual system in λ ; these are the one-level, dual-primal, and all-floating or total FETI methods, see [10, 37, 28]. As mentioned already our presentation concentrates on one-level FETI methods.

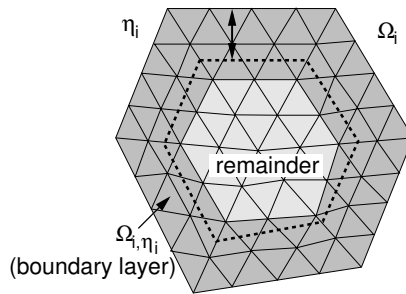


FIGURE 1. Boundary layer Ω_{i, η_i} of the subdomain Ω_i , cf. Definition 2.6.

2.3. Boundary layers. Our analysis will require some notation of a boundary layer near subdomain interfaces. Therefore we need the following definition which is closely related to the one in [15].

Definition 2.6 (discrete boundary layer). For a parameter $\nu > 0$ we define the *discrete boundary layer* $\Omega_{i, \nu}$ by

$$\bar{\Omega}_{i, \nu} := \bigcup \{ \bar{\tau} : \tau \in \mathcal{T}_i, \text{dist}(\tau, \partial\Omega_i) \leq \nu \},$$

i. e., the set of all points which have at most distance ν from the boundary $\partial\Omega_i$, extended to form a union of elements.

An illustration of this definition is given in Fig. 1. Later on in our paper we need the following concept of a finite covering of this boundary layer, which can also be found in [37, Section 3.5] as well as in [15]. For any subdomain boundary layer $\Omega_{i, \nu}$ we can find a finite covering by small shape-regular domains $\{\omega_j^{(i)}\}_j$, in the sequel called *patches*, with $\omega_j^{(i)} \subset \Omega_{i, \nu}$ and $\text{diam} \omega_j^{(i)} \simeq \nu$, as well as $\partial\omega_j^{(i)} \cap \partial\Omega_i \neq \emptyset$. Additionally, we need the following technical assumption later on in our presentation.

Assumption A3. For each subdomain Ω_i the finite covering $\{\omega_j^{(i)}\}_j$ of the boundary layer $\Omega_{i, \nu}$ above can be chosen fulfilling the following properties:

- (i) The patches $\{\omega_j^{(i)}\}_j$ are regular domains in the sense of Definition 2.1.
- (ii) The patches have finite overlap, i. e., the number of patches sharing a point $y \in \Omega_{i, \nu}$ is uniformly bounded.
- (iii) For each patch $\omega_j^{(i)}$ the intersection $\partial\omega_j^{(i)} \cap \partial\Omega_i$ is a union of faces of the patch with its diameter proportional to ν . Furthermore, for any edge $E \in \mathcal{E}_i$ the intersection $\partial\omega_j^{(i)} \cap E$ is a union of edges of the patch $\omega_j^{(i)}$.

For generalisations to more irregular domains in two dimensions see again [9, 20].

We also need to define some quantities related to the coefficient $\alpha(\cdot)$. First, without loss of generality, we assume that the coefficient $\alpha(\cdot)$ is constant on the finite elements of the triangulation \mathcal{T}_i , cf. [15]. Secondly, we define lower and upper bounds of the coefficient on the subdomain boundary layers.

Definition 2.7. For each subdomain let $0 < \eta_i \leq H_i$ be such that $\eta_i \simeq \eta_j$ for all neighbouring subdomains Ω_j . We set

$$\underline{\alpha}_i^{\eta_i} := \min_{x \in \Omega_{i, \eta_i}} \alpha(x), \quad \bar{\alpha}_i^{\eta_i} := \max_{x \in \Omega_{i, \eta_i}} \alpha(x),$$

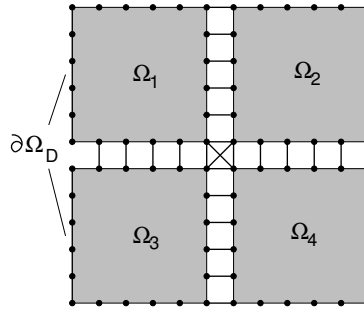


FIGURE 2. One-level FETI constraints, fully redundant, for four subdomains with Dirichlet boundary $\partial\Omega_D$.

such that

$$\underline{\alpha}_i^{\eta_i} \leq \alpha(x) \leq \bar{\alpha}_i^{\eta_i} \quad \text{for } x \in \Omega_{i,\eta_i}.$$

Remark 2.8. It is important to note that the ratio $\bar{\alpha}_i^{\eta_i}/\underline{\alpha}_i^{\eta_i}$ is neither depending on inter-subdomain coefficient jumps nor on the values of $\alpha(\cdot)$ in the interior regions $\Omega_i \setminus \Omega_{i,\eta_i}$. The coefficients $\alpha(\cdot)$ may have arbitrary large jumps across the subdomain interfaces and arbitrary but positive values in the subdomain interiors.

3. FETI METHODS FOR MULTISCALE PDES

In this section we give the formulation of our one-level FETI method for varying coefficients following mainly the approach of Klawonn and Widlund [21] with some modifications which we will point out explicitly (see also [37]).

3.1. Formulation of one-level FETI methods. Following [37, Sect. 6.3], we introduce separate unknowns $u_i \in V^h(\Omega_i)$ on the subdomains, see Figure 2, and denote by $u = [u_1, \dots, u_N]^\top$ the discontinuous approximation of \tilde{u} in $\prod_{i=1}^N V^h(\Omega_i)$. The continuity of the solution is enforced by constraints of the form

$$u_i(x^h) - u_j(x^h) = 0 \quad \text{for } x^h \in \Gamma_{ij}^h.$$

In this work we consider only fully redundant constraints, cf. [37, Sect. 6.3.3]. Let M be the total number of constraints and set $U := \mathbb{R}^M$. Then we can compactly write the constraints as

$$(3.1) \quad Bu := \sum_{i=1}^N B_i u_i = 0,$$

where the jump operators $B_i : V^h(\Omega_i) \rightarrow U$ can be represented as signed Boolean matrices, and $B : \prod_{i=1}^N V^h(\Omega_i) \rightarrow U$ is defined by $B := [B_1 | \dots | B_N]$. We refer to U as the space of Lagrange multipliers and introduce the block notation $K := \text{diag}(K_i)$ and $f := [f_1 | \dots | f_N]^\top$. System (2.4) can now be rewritten as the saddle point system

$$(3.2) \quad \begin{pmatrix} K_1 & & 0 & B_1^\top \\ & \ddots & & \vdots \\ 0 & & K_N & B_N^\top \\ B_1 & \cdots & B_N & 0 \end{pmatrix} \begin{pmatrix} u_1 \\ \vdots \\ u_N \\ \lambda \end{pmatrix} = \begin{pmatrix} f_1 \\ \vdots \\ f_N \\ 0 \end{pmatrix},$$

which is uniquely solvable (up to adding elements from $\ker B^\top$ to λ) if and only if $\ker(K) \cap \ker(B) = \{0\}$. The latter is true whenever the Dirichlet boundary is non-empty.

We introduce the operators $R_i : \mathbb{R} \rightarrow V^h(\Omega_i)$ such that $\text{range } R_i = \ker K_i$ and we set $R := \text{diag}(R_i)$. In particular $R_i \equiv 0$ if Ω_i is non-floating. Let K_i^\dagger denote some pseudo-inverse of K_i . Eliminating the unknowns u_i from (3.2) we obtain that

$$(3.3) \quad u_i = K_i^\dagger [f_i - B_i^\top \lambda] + R_i \xi_i,$$

for some $\xi = [\xi_i]_{i=1}^N$ under the compatibility condition

$$f_i - B_i^\top \lambda \in \text{range } K_i,$$

which is equivalent to

$$R_i^\top (f_i - B_i^\top \lambda) = 0.$$

Both the term $R_i \xi_i$ in (3.3) and the above compatibility condition can be dropped if Ω_i is non-floating. Finally, with the abbreviations

$$F := B K^\dagger B^\top, \quad G := B R, \quad d := B K^\dagger f, \quad e := R^\top f,$$

we arrive at the dual formulation

$$(3.4) \quad \begin{pmatrix} F & -G \\ G^\top & 0 \end{pmatrix} \begin{pmatrix} \lambda \\ \xi \end{pmatrix} = \begin{pmatrix} d \\ e \end{pmatrix}.$$

In practice this system is solved using the projection $P : U \rightarrow \ker G^\top$ defined by

$$(3.5) \quad P := I - Q G (G^\top Q G)^{-1} G^\top,$$

where the SPD operator $Q : U \rightarrow U$ is yet to be specified. Introducing the subspace

$$(3.6) \quad V := \{\lambda \in U : \langle B z, \lambda \rangle = 0 \quad \forall z \in \ker K\},$$

i. e., $V = \ker G^\top = \text{range } P$, the saddle point system (3.4) can be reduced to solving the equation

$$(3.7) \quad P^\top F \tilde{\lambda} = P^\top (d - F \lambda_0),$$

for $\tilde{\lambda} \in V$, where $\lambda_0 = Q G (G^\top Q G)^{-1} e$. The original variables λ and ξ can then be recovered from the relations $\lambda = \lambda_0 + \tilde{\lambda}$ and $\xi = (G^\top Q G)^{-1} G^\top Q (F \lambda - d)$.

Several things are worth mentioning. First note that that $G^\top Q G$ is the Galerkin projection of $B^\top Q B$ onto $\ker K$. Since $\ker K \cap \ker B = \{0\}$, the operator $G^\top Q G$ is invertible as long as Q is SPD on $\text{range } G$. Furthermore, since equation (3.7) is SPD on the subspace V , it can be solved using a preconditioned conjugate gradient method with the preconditioner $P M^{-1}$, where M^{-1} is a preconditioner for F on the subspace V . The actual solution u can finally be recovered using (3.3). Note that even if λ is only unique up to an element from $\ker B^\top$, the solution u is always unique. The crucial ingredients that will make the method robust are the choices of Q and M^{-1} above.

The linear operator $Q : U \rightarrow U$ is chosen as a diagonal matrix. Let $\lambda_{ij}(x^h)$ denote the component of $\lambda \in U$ which corresponds to the constraint $u_i(x^h) - u_j(x^h) = 0$ at the interface node $x^h \in \Gamma_{ij}^h$. We set

$$(3.8) \quad (Q \lambda)_{ij}(x^h) := \min(\bar{\alpha}_i^{\eta_i}, \bar{\alpha}_j^{\eta_j}) q_i(x^h) \lambda_{ij}(x^h),$$

where

$$(3.9) \quad q_i(x^h) := \begin{cases} (1 + \log(H_i/h_i)) \frac{h_i^2}{H_i} & \text{if } x^h \text{ lies on a 3D face,} \\ h_i & \text{if } x^h \text{ lies on a 3D edge/vertex,} \\ (1 + \log(H_i/h_i)) \frac{h_i}{H_i} & \text{if } x^h \text{ lies on a 2D edge,} \\ 1 & \text{if } x^h \text{ is a 2D vertex} \end{cases}$$

(note that $q_i(x^h) \simeq q_j(x^h)$ for neighbouring subdomains since $H_i \simeq H_j$ and $h_i \simeq h_j$). This is a generalisation of the choice given by Klawonn and Widlund [21], with the difference that we use the upper estimates $\bar{\alpha}_i^{\eta_i}$ of $\alpha(\cdot)$ in the discrete boundary layers Ω_{i,η_i} instead of a constant value $\alpha_{|\Omega_i} = \alpha_i$. The fact that this choice of Q uses the upper bounds $\bar{\alpha}_i^{\eta_i}$ at each interface node x^h is for theoretical purposes only. In practice it is of course also possible (and usually more convenient) to use pointwise weights as introduced later on in Section 5 (see also Rixen and Farhat [31, 32]).

In order to define our preconditioner M^{-1} we first define the Schur complement S_i of $K_{i,II}$ in K_i by

$$S_i = K_{i,\Gamma\Gamma} - K_{i,\Gamma I} [K_{i,II}]^{-1} K_{i,I\Gamma},$$

(cf. the grouping introduced in (2.3)) as well as the block operator $S := \text{diag}(S_i)$. Note, that the application of S_i means actually solving a Dirichlet boundary value problem on the subdomain Ω_i . Secondly, we also need to introduce scaling operators D_i for the jump operators B_i . For each subdomain Ω_i , D_i is again a diagonal matrix mapping the space of Lagrange multipliers to itself. We set

$$(D_i \lambda)_{ij}(x^h) := \delta_j^\dagger(x^h) \lambda_{ij}(x^h),$$

with the weighted counting functions

$$(3.10) \quad \delta_j^\dagger(x^h) := \begin{cases} \bar{\alpha}_j^{\eta_j} \left[\sum_{k \in \mathcal{N}_{x^h}} \bar{\alpha}_k^{\eta_k} \right]^{-1} & \text{for } x^h \in \partial\Omega_j^h \cap \Gamma^h, \\ 1 & \text{for } x^h \in \partial\Omega_j^h \cap \partial\Omega^h, \\ 0 & \text{otherwise.} \end{cases}$$

Here, $\mathcal{N}_{x^h} := \{i \in 1, \dots, N : x^h \in \partial\Omega_i\}$, i.e., the index set of the subdomains sharing the node $x^h \in \Gamma^h$. The function $\delta_i^\dagger(\cdot)$ can be interpreted as a finite element function on the skeleton $\partial\Omega \cup \Gamma$, and the union of all these functions provides a partition of unity on the skeleton, cf. [37, Section 6.2.1]. The preconditioner is now chosen to be

$$(3.11) \quad M^{-1} := \sum_{i=1}^N D_i B_i \begin{pmatrix} S_i & 0 \\ 0 & 0 \end{pmatrix} B_i^\top D_i.$$

Again, the choice of $\delta_i^\dagger(\cdot)$ (and thus of D_i and M^{-1}) is a generalisation of the method analysed by Klawonn and Widlund, using the upper bound $\bar{\alpha}_i^{\eta_i}$ instead of a constant value α_i on Ω_i .

Let us summarise the one-level FETI algorithm. To solve system (3.2) (and thus the original FE system (2.4)), we apply a projected preconditioned conjugate gradient method to the Lagrange multiplier system (3.7) with a special initial guess λ_0 . In each step, the application of F essentially means solving local (regularised) Neumann problems, while the application of the preconditioner M^{-1} essentially means solving local Dirichlet problems. The projection steps P and P^\top involve the solution of a coarse problem given by the operator

$G^\top Q G$, which can be interpreted as a weighted graph Laplace operator on the connectivity graph of the subdomains $\{\Omega_i\}$, where each floating subdomain is a node of that graph. In what follows, we assume that these two types of problems, i. e., the local Dirichlet/Neumann problems and the global coarse problem, can be handled by direct solvers, which means that their condition numbers (which will usually be large due to the coefficient variations) do not effect the solves. Note, that the fact that the Lagrange multiplier λ is only unique up to an element in $\ker B^\top$ does not result in any principal mathematical and implementational difficulties [21, 29].

3.2. Analysis of the one-level FETI method. The convergence of CG depends on the condition number κ of the preconditioned operator $P M^{-1} P^\top F : V \rightarrow V$. It is well-known that the energy norm of the error decreases at least by a factor $2\left(\frac{\sqrt{\kappa}-1}{\sqrt{\kappa}+1}\right)$ in each CG iteration. Thus, we are interested in bounding κ . The key result of the paper (Theorem 3.3 below) gives such a bound for the variant of one-level FETI described in Section 3.1. Our analysis follows in large parts the analysis in [21, 37]. In particular we work in the space $V_{/\ker B^\top}$, i. e., the quotient space of V with respect to $\ker B^\top$. Furthermore, as usual in iterative substructuring methods, we will have to work with trace spaces and discrete harmonic functions. First, we define spaces on the local boundaries and the corresponding product space, i. e.,

$$(3.12) \quad W_i := \{v_i|_{\partial\Omega_i} : v_i \in V^h(\Omega_i)\}, \quad W := \prod_{i=1}^N W_i,$$

and regard S_i as an operator mapping W_i to W_i , and $S : W \rightarrow W$. Secondly, we define

$$(3.13) \quad \begin{aligned} (\ker S_i)^\perp &:= \{w_i \in W_i : (w_i, z)_{L^2(\partial\Omega_i)} = 0 \quad \forall z \in \ker S_i\}, \\ (\ker S)^\perp &:= \{w \in W : w_i \in (\ker S_i)^\perp\}. \end{aligned}$$

Moreover, we define the seminorm $|w_i|_{S_i} := \langle S_i w_i, w_i \rangle^{1/2}$ on $V^h(\partial\Omega_i)$ which has the property that $|w_i + c|_{S_i} = |w_i|_{S_i}$ for any constant $c \in \mathbb{R}$. On the product space W we introduce the seminorm $|w|_S := (\sum_{i=1}^N |w_i|_{S_i}^2)^{1/2}$. Finally, we define the space $V' = \text{range } P^\top$ by

$$V' := \{\mu \in U : \langle B z, Q \mu \rangle = 0 \quad \forall z \in \ker K\},$$

which is isomorphic to V in (3.6). Using the fact that Q is SPD on $\text{range } G$ and that the operator

$$(3.14) \quad P_D := [B_1^\top D_1 B_1 | \dots | B_N^\top D_N B_N]$$

is a projection fulfilling $B P_D = B$, one can show that M^{-1} is SPD on the quotient space $V'_{/\ker B^\top}$, cf. [21]. Hence, there exists a well-defined inverse M mapping $V'_{/\ker B^\top}$ to itself. As usual in the analysis of one-level FETI methods, we show spectral bounds of the form

$$(3.15) \quad \langle M \lambda, \lambda \rangle \leq \langle F \lambda, \lambda \rangle \leq C^* \langle M \lambda, \lambda \rangle \quad \forall \lambda \in V'_{/\ker B^\top},$$

which imply the condition number estimate $\kappa \leq C^*$ (cf. [37, Sect. 6.3]). To do so, we need the following characterisations of $\langle M \cdot, \cdot \rangle$, $\langle M^{-1} \cdot, \cdot \rangle$ and the space V' which can be found in [37, Sect. 6.3]:

(i) The projection $P_D : W \rightarrow W$ fulfils the identity

$$(3.16) \quad (P_D w)_i(x^h) = \sum_{j \in \mathcal{N}_{x^h}} \delta_j^\dagger(x^h) [w_i(x^h) - w_j(x^h)] \quad \text{for } x^h \in \partial\Omega_i^h.$$

(ii) From the definition (3.11) of M^{-1} we see that for $\mu_w := B w$,

$$(3.17) \quad \langle M^{-1} \mu_w, \mu_w \rangle = |P_D w|_S^2.$$

(iii) A standard duality argument yields

$$(3.18) \quad \langle F \lambda, \lambda \rangle = \sup_{w \in (\ker S)^\top} \frac{\langle \lambda, B w \rangle^2}{|w|_S^2}, \quad \langle M \lambda, \lambda \rangle = \sup_{\mu \in V'} \frac{\langle \lambda, \mu \rangle^2}{\langle M^{-1} \mu, \mu \rangle}.$$

(iv) We also have the following characterisation of the space V' (cf. [37, Lemma 6.12]).

Lemma 3.1. *For any $w \in W$, there exists a unique $z_w \in \ker S$ such that $B(w + z_w) \in V'$. Moreover,*

$$\|B z_w\|_Q \leq \|B w\|_Q,$$

where $\|\mu\|_Q := \langle \mu, Q \mu \rangle^{1/2}$.

It is worth mentioning that $z_w = \operatorname{argmin}_{z \in \ker S} \|B(w + z)\|_Q$ and that the mapping $w \mapsto z_w$ is linear (see [29, 30]).

Note that the lower bound in (3.15) can be shown by algebraic arguments [37, Theorem 6.15] independently of our particular choices of Q and M^{-1} . The upper bound in (3.15) relies on similar algebraic arguments and the crucial estimate

$$(3.19) \quad |P_D(w + z_w)|_S^2 \leq C^* |w|_S^2 \quad \forall w \in (\ker S)^\perp.$$

where $z_w \in \ker S$ is uniquely determined by w due to Lemma 3.1.

It was shown by Klawonn and Widlund [21] (see also [37, Theorem 6.15]) that for regular subdomains and piecewise constant coefficients, the constant C^* is independent of the values of $\alpha(\cdot)$ and depends only on $\max_{i=1, \dots, N} (1 + \log(H_i/h_i))^2$. In particular, the estimate is robust with respect to jumps of the coefficients across subdomain interfaces. The following lemma shows a similar estimate in the case of an arbitrary positive coefficient function $\alpha \in L^\infty(\Omega)$.

Lemma 3.2. *Let $\eta_i, \underline{\alpha}_i^{\eta_i}, \bar{\alpha}_i^{\eta_i}, i = 1, \dots, N$ be defined according to Definition 2.7. Then*

$$|P_D(w + z_w)|_S^2 \lesssim \max_{k=1}^N \left(\frac{H_k}{\eta_k} \right)^2 \max_{i=1}^N \frac{\bar{\alpha}_i^{\eta_i}}{\underline{\alpha}_i^{\eta_i}} (1 + \log(H_i/h_i))^2 |w|_S^2 \quad \forall w \in (\ker S)^\perp.$$

If in addition $\alpha(x) \gtrsim \underline{\alpha}_i^{\eta_i}$ for all $x \in \Omega_i$ and for all $i = 1, \dots, N$, we have the improved estimate

$$|P_D(w + z_w)|_S^2 \lesssim \max_{k=1}^N \frac{H_k}{\eta_k} \max_{i=1}^N \frac{\bar{\alpha}_i^{\eta_i}}{\underline{\alpha}_i^{\eta_i}} (1 + \log(H_i/h_i))^2 |w|_S^2 \quad \forall w \in (\ker S)^\perp,$$

with a linear instead of quadratic dependency on H_k/η_k .

Proof. Postponed to Section 4.3. □

Our main result on the conditioning of our one-level FETI methods is summarised in the following theorem.

Theorem 3.3. *Let $\eta_i, \underline{\alpha}_i^{\eta_i}, \bar{\alpha}_i^{\eta_i}, i = 1, \dots, N$ be defined according to Definition 2.7. Then the one-level FETI preconditioner defined in (3.11) satisfies the condition number estimate*

$$\kappa(P M^{-1} P^\top F) \lesssim \max_{i=k}^N \left(\frac{H_k}{\eta_k} \right)^\beta \max_{i=1}^N \frac{\bar{\alpha}_i^{\eta_i}}{\underline{\alpha}_i^{\eta_i}} (1 + \log(H_i/h_i))^2.$$

In general, $\beta \leq 2$. Under the stronger assumption

$$\alpha(x) \gtrsim \underline{\alpha}_i^{\eta_i} \quad \forall x \in \Omega_i \quad \forall i = 1, \dots, N,$$

we have the improved estimate with $\beta \leq 1$. These statements hold in both two and three dimensions.

Proof. The proof is of the same structure as the one of [37, Theorem 6.15] and follows directly from the previous considerations, i. e., (3.15), (3.17), (3.18), Lemma 3.1, and the estimates in Lemma 3.2. \square

Remark 3.4. There are two special cases of Theorem 3.3 concerning α and the parameters η_i .

- (i) For the case that $\alpha(\cdot)$ is piecewise constant on the subdomains, Theorem 3.3 reproduces the known result by Klawonn and Widlund [21]. This is because $\underline{\alpha}_i^{H_i} = \overline{\alpha}_i^{H_i} \equiv \alpha|_{\Omega_i}$.
- (ii) If the η_i can be chosen with $\eta_i \simeq H_i$ and $\alpha(x) \leq C_\eta \alpha(y)$ for $x, y \in \Omega_{i, \eta_i}$ for each $i = 1, \dots, N$, then we obtain the condition number bound $C_\eta (1 + \log(H/h))^2$, i. e., the method is completely robust to possible coefficient variation in $\Omega_i \setminus \Omega_{i, \eta_i}$.

Remark 3.5. In our analysis we will never use the values of the coefficient $\alpha(\cdot)$ in the subdomain interiors, i. e., any positive values in $(0, \infty)$ are possible. It is therefore interesting to consider also the following two limit cases which correspond to applying our FETI methods to (homogeneous) problems on perforated domains (e. g. bubbly flow).

- (i) The case that the coefficient in the subdomain interiors goes to infinity corresponds to Dirichlet boundary conditions on $\partial\Omega_{i, \eta_i} \setminus \partial\Omega_i$, see e. g. [1]. We obtain the condition number bound as in Theorem 3.3 with $\beta = 1$.
- (ii) The case that the coefficient vanishes completely in $\Omega_i \setminus \Omega_{i, \eta_i}$ corresponds to Neumann boundary conditions on $\partial\Omega_{i, \eta_i} \setminus \partial\Omega_i$. Thus in this case we obtain the condition number bound as in Theorem 3.3 with $\beta = 2$.

It remains to prove Lemma 3.2.

4. PROOF OF THE THEORETICAL RESULTS

In the first three subsections of this section we provide some technical tools which we need for the proof of Lemma 3.2. The analysis is carried out in the spaces W_i which can be interpreted as spaces of discrete α -harmonic functions, since for all $v \in W_i$,

$$(4.1) \quad |v|_{S_i}^2 = \min \left\{ \int_{\Omega_i} \alpha_i |\nabla \tilde{v}|^2 dx : \tilde{v} \in V^h(\Omega_i), \tilde{v}|_{\partial\Omega_i} = v \right\}.$$

The function $\mathcal{H}_\alpha v$ for which the minimum is attained is called the *discrete α -harmonic extension* of $v \in V^h(\partial\Omega_i)$ to $V^h(\Omega_i)$. For convenience, we also define the discrete trace seminorm for $v \in W_i$,

$$(4.2) \quad |v|_{H^{1/2}(\partial\Omega_i)}^2 := \min \left\{ \int_{\Omega_i} |\nabla \tilde{v}|^2 dx : \tilde{v} \in V^h(\Omega_i), \tilde{v}|_{\partial\Omega_i} = v \right\}.$$

This seminorm vanishes for constant functions. The function $\mathcal{H}v$ for which the minimum in (4.2) is attained is called *discrete harmonic extension* of v from $\partial\Omega_i$ to Ω_i . We use two main tools for our analysis which are interesting on their own.

As a first tool, in Section 4.1 we show an estimate of the form

$$(4.3) \quad |v|_{S_i}^2 \lesssim \overline{\alpha}_i^{\eta_i} \left\{ |v|_{H^{1/2}(\partial\Omega_i)}^2 + \frac{1}{\eta_i} \|v\|_{L^2(\partial\Omega_i)}^2 \right\},$$

using a cut-off function which vanishes on the interior $\Omega_i \setminus \Omega_{i,\eta_i}$. This technique is closely related to an approach in [15] for analysing overlapping Schwarz methods for multiscale problems. This result allows us (i) to remove the dependency on $\alpha(\cdot)$ in the interior of the subdomain completely, and (ii) to reuse the known FETI tools which are carried out in $H^{1/2}$ -seminorms. The price to pay is a factor of $1/\eta_i$ in front of the L^2 -term instead of $1/H_i$ in the piecewise constant case. This will lead to a factor H_i/η_i in the condition number estimate.

In the case where $\alpha(\cdot)$ is completely arbitrary in the interior (in particular not bounded from below by $\underline{\alpha}_i^{\eta_i}$), we need a second tool. We estimate the L^2 -term in (4.3) from above by the H^1 -seminorm of v , but restricted to the boundary layer Ω_{i,η_i} . That means, we need Poincaré- and Friedrichs-type inequalities on boundary layer domains (which are topologically non-trivial) with explicit information on the dependency of the Poincaré/Friedrichs constant on the aspect ratio H_i/η_i . It turns out that the dependency is linear in H_i/η_i which leads to the second factor in the condition number estimate. A direct proof of Friedrichs' inequality for so-called N -point connected domains (a generalisation of star-shaped domains) can be found, e. g., in a recent work by Weiyang and He [40]. However, in addition to the usual Poincaré and Friedrichs inequality, we also need discrete estimates similar to the ones in [37, Section 4.6] (see also [3]). We generalise the idea given in [40] to show all the needed inequalities in Section 4.2. Section 4.3 contains finally the proof of Lemma 3.2.

Throughout the whole section we make use of the nodal interpolator I^h onto $V^h(\Omega_i)$ (resp. $V^h(\partial\Omega_i)$) which is continuous in the H^1 -seminorm (resp. $H^{1/2}$ -seminorm) and in the L^2 -norm for quadratic functions. See [37, Lemma 3.9].

4.1. Cut-off techniques.

Lemma 4.1. *For all $v \in V^h(\partial\Omega_i)$ we have*

$$(i) \quad |v|_{S_i}^2 \lesssim \bar{\alpha}_i^{\eta_i} \left\{ |\tilde{v}|_{H^1(\Omega_{i,\eta_i})}^2 + \frac{1}{\eta_i} \|v\|_{L^2(\partial\Omega_i)}^2 \right\},$$

$$(ii) \quad |v|_{S_i}^2 \lesssim \bar{\alpha}_i^{\eta_i} \left\{ |v|_{H^{1/2}(\partial\Omega_i)}^2 + \frac{1}{\eta_i} \|v\|_{L^2(\partial\Omega_i)}^2 \right\},$$

where \tilde{v} is an arbitrary extension of v from $V^h(\partial\Omega_i)$ to $V^h(\Omega_i)$.

Proof. We can find a discrete cut-off function $\chi \in V^h(\Omega_i)$ with

- $\chi(x) \in [0, 1]$,
- $\chi|_{\partial\Omega_i} = 1$,
- $\chi|_{\Omega_i \setminus \Omega_{i,\eta_i}} = 0$, and
- $\|\nabla\chi\|_{L^\infty(\Omega_i)} \lesssim \eta_i^{-1}$.

These properties can, e. g., be obtained by defining $\chi \in V^h(\Omega_i)$ at each node $x^h \in \Omega_i^h$ by

$$\chi(x^h) = \begin{cases} 1 - \text{dist}(x^h, \partial\Omega_i)/\eta_i & \text{for } \text{dist}(x^h, \partial\Omega_i) \leq \eta_i, \\ 0 & \text{else.} \end{cases}$$

For more details see [29].

Let $v \in V^h(\partial\Omega_i)$ and let $\tilde{v} \in V^h(\Omega_i)$ denote an arbitrary extension of v from $\partial\Omega_i$ to Ω_i . Then, $I^h(\chi\tilde{v}) \in V^h(\Omega_i)$ is also an extension of v from $\partial\Omega_i$ to Ω_i , and because of the minimum

property (4.1) we can bound the S_i -energy norm of v by the α -weighted H^1 -seminorm of $I^h(\chi \tilde{v})$. Using the continuity of the nodal interpolator I^h we obtain

$$\begin{aligned}
|v|_{S_i}^2 &\leq \int_{\Omega_i} \alpha(x) \underbrace{|\nabla[I^h(\chi \tilde{v})(x)]|^2}_{0 \text{ in } \Omega_i \setminus \Omega_{i, \eta_i}} dx = \int_{\Omega_{i, \eta_i}} \alpha(x) \left| \nabla[I^h(\chi(x) \tilde{v}(x))] \right|^2 dx \\
(4.4) \quad &\leq \int_{\Omega_{i, \eta_i}} \bar{\alpha}_i^{\eta_i} \left| \nabla[I^h(\chi(x) \tilde{v}(x))] \right|^2 dx \lesssim \bar{\alpha}_i^{\eta_i} \int_{\Omega_{i, \eta_i}} |\nabla(\chi(x) \tilde{v}(x))|^2 dx \\
&\lesssim \bar{\alpha}_i^{\eta_i} \left\{ \underbrace{\|\nabla \chi\|_{L^\infty(\Omega_i)}^2}_{\lesssim \eta_i^{-2}} \|\tilde{v}\|_{L^2(\Omega_{i, \eta_i})}^2 + \underbrace{\|\chi\|_{L^\infty(\Omega_i)}^2}_{=1} \|\nabla \tilde{v}\|_{L^2(\Omega_{i, \eta_i})}^2 \right\}.
\end{aligned}$$

As in the proof of [37, Lemma 3.10] we cover the boundary layer Ω_{i, η_i} by regular patches $\{\omega_j\}_j$ which satisfy Assumption A3. We have, trivially,

$$(4.5) \quad \frac{1}{\eta_i^2} \|\tilde{v}\|_{L^2(\Omega_{i, \eta_i})}^2 \leq \sum_j \frac{1}{\eta_i^2} \|\tilde{v}\|_{L^2(\omega_j)}^2.$$

Due to Assumption A3, for each j the intersection $\partial\omega_j \cap \partial\Omega_i$ is a union of shape-regular faces of the patch ω_j with its diameter proportional to η_i . Thus, we can apply a Friedrichs-type inequality [37, Lemma A.6] on each patch ω_j which yields

$$(4.6) \quad \sum_j \frac{1}{\eta_i^2} \|\tilde{v}\|_{L^2(\omega_j)}^2 \lesssim \sum_j \left\{ \|\tilde{v}\|_{H^1(\omega_j)}^2 + \frac{1}{\eta_i} \|\tilde{v}\|_{L^2(\partial\omega_j \cap \partial\Omega_i)}^2 \right\}.$$

Since the patches have finite overlap, combining (4.4)–(4.6), we easily obtain (i). Choosing \tilde{v} to be the discrete harmonic extension $\mathcal{H}v$, we also obtain estimate (ii). \square

The following cut-off functions (cf. [37, Section 4.6]) are also needed for the proofs below.

Definition 4.2 (Finite element cut-off functions). Let Ω_i be one of the subdomains. For a vertex $V \in \mathcal{V}_i$ we define the finite element function $\theta_V \in V^h(\partial\Omega_i)$ as the trace of the usual nodal basis function associated to the vertex V , i. e. $\theta_V(x)$ equals 1 on V and vanishes on all other nodes in $\partial\Omega_i^h$. For an edge $E \in \mathcal{E}_i$ we define $\theta_E \in V^h(\partial\Omega_i)$ by the finite element function which equals 1 on all (interior) nodes of the edge E and vanishes on all other nodes. Similarly, for a face $F \in \mathcal{F}_i$ the function $\theta_F \in V^h(\partial\Omega_i)$ equals 1 on all interior nodes of the face F and vanishes elsewhere.

For a simplified notation we set $\mathcal{X}_i := \mathcal{V}_i \cup \mathcal{E}_i \cup \mathcal{F}_i$, where in two dimensions we drop the faces. The family of functions $\{\theta_X\}_{X \in \mathcal{X}_i}$ provides a partition of unity on $\partial\Omega_i$ in the sense that

$$v = \sum_{X \in \mathcal{X}_i} I^h(\theta_X v) \quad \forall v \in V^h(\partial\Omega_i).$$

4.2. Generalised Poincaré, Friedrichs, and discrete Sobolev-type inequalities. Let Ω_i be a regular domain and let

$$(4.7) \quad 0 < \eta_i \leq H_i.$$

In the following we consider the boundary layer Ω_{i, η_i} of Ω_i (cf. Definition 2.6). We provide Poincaré, Friedrichs, and Sobolev-type inequalities on Ω_{i, η_i} making explicit the dependency of the respective constants on the aspect ratio H_i/η_i .

Lemma 4.3 (generalised Poincaré inequality). *Suppose $u \in H^1(\Omega_i, \eta_i)$. Let $\tilde{\Gamma}$ be either (a) an edge of Ω_i (in two dimensions), (b) a face of Ω_i (in three dimensions), or (c) the entire boundary $\partial\Omega_i$ of Ω_i . Then*

$$(4.8) \quad \frac{1}{H_i} \|u\|_{L^2(\partial\Omega_i)}^2 \lesssim \frac{H_i}{\eta_i} |u|_{H^1(\Omega_i, \eta_i)}^2 + H_i^{d-2} \left(\frac{1}{|\tilde{\Gamma}|} \int_{\tilde{\Gamma}} u(x) ds_x \right)^2.$$

Proof. Postponed to the Appendix. □

Corollary 4.4 (generalised Friedrichs inequality). *Suppose $u \in H^1(\Omega_i, \eta_i)$. Let $\tilde{\Gamma} \subset \partial\Omega_i$ be an edge of Ω_i (in two dimensions) or a face of Ω_i (in three dimensions). If $u|_{\tilde{\Gamma}} = 0$ then*

$$(4.9) \quad \frac{1}{H_i} \|u\|_{L^2(\partial\Omega_i)}^2 \leq C \frac{H_i}{\eta_i} |u|_{H^1(\Omega_i, \eta_i)}^2.$$

Proof. Follows directly from Lemma 4.3. □

Lemma 4.5 (generalised discrete Sobolev-type inequality). *Suppose $u \in V^h(\Omega_i, \eta_i)$.*

- (i) *Let $\Omega_i \subset \mathbb{R}^2$ and let $\zeta(u)$ be (a) a nodal evaluation of u in $\partial\Omega_i$, (b) the average value of u over an edge E of Ω_i , or (c) the average of u over the entire boundary $\partial\Omega_i$. Then*

$$(4.10) \quad \|u - \zeta(u)\|_{L^\infty(\partial\Omega_i)}^2 \lesssim \frac{H_i}{\eta_i} \left(1 + \log \frac{\eta_i}{h_i}\right) |u|_{H^1(\Omega_i, \eta_i)}^2.$$

$$(4.11) \quad \frac{1}{H_i} \|u - \zeta(u)\|_{L^2(\partial\Omega_i)}^2 \lesssim \frac{H_i}{\eta_i} \left(1 + \log \frac{\eta_i}{h_i}\right) |u|_{H^1(\Omega_i, \eta_i)}^2.$$

- (ii) *Let $\Omega_i \subset \mathbb{R}^3$ and let $\zeta(u)$ be the average value of u over (a) an edge E of Ω_i , (b) a face F of Ω_i , or (c) all of $\partial\Omega_i$. Then, for all edges E' of Ω_i ,*

$$(4.12) \quad \|u - \zeta(u)\|_{L^2(E')}^2 \lesssim \frac{H_i}{\eta_i} \left(1 + \log \frac{\eta_i}{h_i}\right) |u|_{H^1(\Omega_i, \eta_i)}^2,$$

$$(4.13) \quad \frac{1}{H_i} \|u - \zeta(u)\|_{L^2(\partial\Omega_i)}^2 \lesssim \frac{H_i}{\eta_i} \left(1 + \log \frac{\eta_i}{h_i}\right) |u|_{H^1(\Omega_i, \eta_i)}^2.$$

Proof. Similar to the proof of Lemma 4.3. For details see the Appendix. □

Remark 4.6. For η_i chosen such that $\Omega_{i, \eta_i} = \Omega_i$, i. e. $H_i/\eta_i \simeq 1$, Lemma 4.3, Corollary 4.4 and Lemma 4.5 reproduce the known Poincaré-, Friedrichs-, and discrete Sobolev-type inequalities, see e. g. [37, Sect. A.4, Lemma 4.15, Lemma 4.16, and Lemma 4.21].

4.3. Proof of Lemma 3.2. We only give a detailed proof for the three-dimensional case. We have to show that

$$(4.14) \quad |P_D(w + z_w)|_S^2 \lesssim \left\{ \max_{k=1}^N \left(\frac{H_k}{\eta_k} \right)^\beta \max_{i=1}^N \frac{\bar{\alpha}_i^{\eta_i}}{\underline{\alpha}_i^{\eta_i}} (1 + \log(H_i/h_i))^2 \right\} |w|_S^2 \quad \forall w \in (\ker S)^\perp,$$

with $\beta = 2$ in general and $\beta = 1$ if $\alpha(x) \gtrsim \underline{\alpha}_i^{\eta_i}$ for all $x \in \Omega_i$ and for all $i = 1, \dots, N$. As in the article [21] by Klawonn and Widlund we split the left hand side into two parts

$$|P_D(w + z_w)|_S^2 \lesssim |P_D w|_S^2 + |P_D z_w|_S^2,$$

and treat them separately.

4.3.1. *Estimating $P_D w$.* We prove that for all $w \in (\ker S)^\perp$,

$$(4.15) \quad |P_D w|_S^2 = \sum_{i=1}^N |(P_D w)_i|_{S_i}^2 \lesssim \max_{j=1}^N \left\{ \left(\frac{H_j}{\eta_j} \right)^\beta \frac{\bar{\alpha}_j^{\eta_j}}{\underline{\alpha}_j} (1 + \log(H_j/h_j))^2 \right\} \sum_{i=1}^N |w_i|_{S_i}^2.$$

By Lemma 4.1(ii), formula (3.16) and the partition of unity on $\partial\Omega_i$ provided by the cut-off functions θ_X from Definition 4.2, we obtain

$$\begin{aligned} |(P_D w)_i|_{S_i}^2 &\lesssim \bar{\alpha}_i^{\eta_i} \left\{ |(P_D w)_i|_{H^{1/2}(\partial\Omega_i)}^2 + \frac{1}{\eta_i} \|(P_D w)_i\|_{L^2(\partial\Omega_i)}^2 \right\} \\ &\lesssim \sum_{X \in \mathcal{X}_i} \sum_{j \in \mathcal{N}_X} \bar{\alpha}_i^{\eta_i} \left\{ |I^h(\theta_X \delta_j^\dagger(w_i - w_j))|_{H^{1/2}(\partial\Omega_i)}^2 + \frac{1}{\eta_i} \|I^h(\theta_X \delta_j^\dagger(w_i - w_j))\|_{L^2(\partial\Omega_i)}^2 \right\} \end{aligned}$$

where $\mathcal{N}_X := \{j : X \subset \partial\Omega_j\}$ for $X \in \mathcal{X}_i$. Using the elementary inequality

$$\bar{\alpha}_i^{\eta_i} [\delta_j^\dagger(x)]^2 \leq \min(\bar{\alpha}_i^{\eta_i}, \bar{\alpha}_j^{\eta_j}),$$

cf. [37], the fact that $\delta_j^\dagger(\cdot)$ is constant on edges and faces, and the fact that $\eta_i \simeq \eta_j$ for neighbouring subdomains, we can show that

$$(4.16) \quad |(P_D w)_i|_{S_i}^2 \lesssim \sum_{X \in \mathcal{X}_i} \sum_{j \in \mathcal{N}_X} \left\{ |\psi_{ij}^X|_{H^{1/2}(\partial\Omega_i)}^2 + \frac{1}{\eta_i} \|\psi_{ij}^X\|_{L^2(\partial\Omega_i)}^2 \right\}$$

where $\psi_{ij}^X := \min(\bar{\alpha}_i^{\eta_i}, \bar{\alpha}_j^{\eta_j})^{1/2} I^h(\theta_X(w_i - w_j))$.

Recall that $\mathcal{X}_i = \mathcal{V}_i \cup \mathcal{E}_i \cup \mathcal{F}_i$. We will now derive in detail, bounds of the form

$$(4.17) \quad |\psi_{ij}^X|_{H^{1/2}(\partial\Omega_i)}^2 + \frac{1}{\eta_i} \|\psi_{ij}^X\|_{L^2(\partial\Omega_i)}^2 \lesssim (1 + \log(H_i/h_i))^2 \sum_{k=i,j} \left(\frac{H_k}{\eta_k} \right)^\beta \frac{\bar{\alpha}_k^{\eta_k}}{\underline{\alpha}_k} |w_k|_{S_k}^2.$$

Due to the regularity of our subdomain partition, each subdomain has a bounded number of faces, edges, and vertices, and each face, edge and vertex is only shared by a bounded number of subdomains. Therefore, (4.16) and (4.17) imply the desired estimate (4.15).

It remains to prove (4.17) for each $X \in \mathcal{X}_i$. We start with the face terms.

Face terms: Let $F \in \mathcal{F}_i \cap \mathcal{F}_j$ and let $\bar{w}_k := 1/|\partial\Omega_k| \int_{\partial\Omega_k} w_k(x) ds_x$, i.e. the average of w_k over Ω_k . First, note that $|I^h(\theta_F(w_j - \bar{w}_j))|_{H^{1/2}(\partial\Omega_i)}^2 \lesssim |I^h(\theta_F(w_j - \bar{w}_j))|_{H^{1/2}(\partial\Omega_j)}^2$. This is because the discrete harmonic extensions from F to Ω_i and Ω_j are equivalent in the corresponding H^1 -seminorms.¹ Applying [37, Lemma 4.24 and Lemma 4.25] and the fact that $H_i \simeq H_j$ for neighbouring subdomains we get

$$\begin{aligned} |\psi_{ij}^F|_{H^{1/2}(\partial\Omega_i)}^2 &\lesssim \min(\bar{\alpha}_i^{\eta_i}, \bar{\alpha}_j^{\eta_j}) |I^h(\theta_F(w_i - \bar{w}_i)) - I^h(\theta_F(w_j - \bar{w}_j)) + I^h(\theta_F(\bar{w}_i - \bar{w}_j))|_{H^{1/2}(\partial\Omega_i)}^2 \\ &\lesssim \min(\bar{\alpha}_i^{\eta_i}, \bar{\alpha}_j^{\eta_j}) (1 + \log(H_i/h_i))^2 \sum_{k=i,j} \left\{ |w_k - \bar{w}_k|_{H^{1/2}(\partial\Omega_k)}^2 + \frac{1}{H_k} \|(w_k - \bar{w}_k)\|_{L^2(\partial\Omega_k)}^2 \right\} + \\ (4.18) \quad &+ \min(\bar{\alpha}_i^{\eta_i}, \bar{\alpha}_j^{\eta_j}) (1 + \log(H_i/h_i)) \underbrace{H_i (|\bar{w}_i|^2 + |\bar{w}_j|^2)}_{\lesssim \frac{1}{H_i} \|w_i\|_{L^2(\partial\Omega_i)}^2 + \frac{1}{H_j} \|w_j\|_{L^2(\partial\Omega_j)}^2}. \end{aligned}$$

¹This equivalence can be shown using a discrete trace inequality or using an extension theorem (see, e.g., [11, Section 5.4]) and the Scott-Zhang interpolation operator [36].

Now continuing this estimate and grouping with respect to i and j we get

$$(4.19) \quad \begin{aligned} |\psi_{ij}^F|_{H^{1/2}(\partial\Omega_i)}^2 &\lesssim (1 + \log(H_i/h_i))^2 \sum_{k=i,j} \bar{\alpha}_k^{\eta_k} \left\{ |w_k|_{H^{1/2}(\partial\Omega_k)}^2 + \frac{1}{H_k} \|w_k - \bar{w}_k\|_{L^2(\partial\Omega_k)}^2 \right\} + \\ &+ (1 + \log(H_i/h_i)) \sum_{k=i,j} \bar{\alpha}_k^{\eta_k} \frac{1}{H_k} \|w_k\|_{L^2(\partial\Omega_k)}^2. \end{aligned}$$

Also, using the L^2 -continuity of the nodal interpolator I^h , Definition 4.2, and the fact that $\eta_i \simeq \eta_j$ for neighbouring subdomains yields

$$(4.20) \quad \frac{1}{\eta_i} \|\psi_{ij}^F\|_{L^2(\partial\Omega_i)}^2 \lesssim \frac{\bar{\alpha}_i^{\eta_i}}{\eta_i} \|w_i\|_{L^2(\partial\Omega_i)}^2 + \frac{\bar{\alpha}_j^{\eta_j}}{\eta_j} \|w_j\|_{L^2(\partial\Omega_j)}^2.$$

Thus to complete the proof of (4.17) we have to bound the norms $|w_k|_{H^{1/2}(\partial\Omega_k)}^2$, $\|w_k - \bar{w}_k\|_{L^2(\partial\Omega_k)}^2$ and $\|w_k\|_{L^2(\partial\Omega_k)}^2$ in (4.19) and (4.20) in terms of $|w_k|_{S_k}^2$, for $k = i, j$.

As above let $\mathcal{H}_\alpha(w_k - \bar{w}_k)$ denote the discrete $\alpha(\cdot)$ -harmonic extension of $w_k - \bar{w}_k$ from $\partial\Omega_k$ to Ω_k which satisfies

$$(4.21) \quad \int_{\Omega_i} \alpha(x) |\nabla \mathcal{H}_\alpha(w_i - \bar{w}_i)(x)|^2 dx = |w_i - \bar{w}_i|_{S_i}^2 = |w_i|_{S_i}^2.$$

Firstly, applying Lemma 4.1(i) with coefficient $\alpha' \equiv 1$ to bound $|w_k - \bar{w}_k|_{H^{1/2}(\partial\Omega_k)}^2$ we conclude that

$$|w_k|_{H^{1/2}(\partial\Omega_k)}^2 = |w_k - \bar{w}_k|_{H^{1/2}(\partial\Omega_k)}^2 \lesssim |\mathcal{H}_\alpha(w_k - \bar{w}_k)|_{H^1(\Omega_k, \eta_k)}^2 + \frac{1}{\eta_k} \|w_k - \bar{w}_k\|_{L^2(\partial\Omega_k)}^2.$$

Secondly, applying Lemma 4.3 (the generalised Poincaré inequality) to $u = \mathcal{H}_\alpha(w_k - \bar{w}_k)$ yields

$$(4.22) \quad \|w_k - \bar{w}_k\|_{L^2(\partial\Omega_k)}^2 \lesssim \frac{H_k^2}{\eta_k} |\mathcal{H}_\alpha(w_k - \bar{w}_k)|_{H^1(\Omega_k, \eta_k)}^2.$$

Finally to bound $\|w_k\|_{L^2(\partial\Omega_k)}^2$ we can apply the discrete Sobolev-type inequality in Lemma 4.5(ii) to $u = \mathcal{H}_\alpha w_k$: If the subdomain Ω_k is floating, we know that $\int_{\partial\Omega_k} w_k(x) ds_x = (w_k, \mathbf{1})_{L^2(\partial\Omega_k)} = 0$ because $w_k \in (\ker S_k)^\perp$. If Ω_k is non-floating w_k vanishes at least at one edge of $\partial\Omega_k$. Thus we can conclude from Lemma 4.5(ii) that

$$(4.23) \quad \|w_k\|_{L^2(\partial\Omega_k)}^2 \lesssim \frac{H_k^2}{\eta_k} (1 + \log(\eta_k/h_k)) |\mathcal{H}_\alpha w_k|_{H^1(\Omega_k, \eta_k)}^2.$$

Note that $|\mathcal{H}_\alpha(w_k - \bar{w}_k)|_{H^1(\Omega_k, \eta_k)}^2 = |\mathcal{H}_\alpha w_k|_{H^1(\Omega_k, \eta_k)}^2$. Hence, by combining (4.19)–(4.23) and by using the fact that $\eta_k \leq H_k$ we get

$$\begin{aligned}
(4.24) \quad & |\psi_{ij}^F|_{H^{1/2}(\partial\Omega_i)}^2 + \frac{1}{\eta_i} \|\psi_{ij}^F\|_{L^2(\partial\Omega_i)}^2 \lesssim (1 + \log(H_i/h_i))^2 \sum_{k=i,j} \left(\frac{H_k}{\eta_k}\right)^2 \bar{\alpha}_k^{\eta_k} |\mathcal{H}_\alpha w_k|_{H^1(\Omega_k, \eta_k)}^2 \\
& = (1 + \log(H_i/h_i))^2 \sum_{k=i,j} \left(\frac{H_k}{\eta_k}\right)^2 \frac{\bar{\alpha}_k^{\eta_k}}{\underline{\alpha}_k^{\eta_k}} \int_{\Omega_k, \eta_k} \underline{\alpha}_k^{\eta_k} |\nabla \mathcal{H}_\alpha w_k|^2 dx \\
& \leq (1 + \log(H_i/h_i))^2 \sum_{k=i,j} \left(\frac{H_k}{\eta_k}\right)^2 \frac{\bar{\alpha}_k^{\eta_k}}{\underline{\alpha}_k^{\eta_k}} \int_{\Omega_k} \alpha(x) |\nabla \mathcal{H}_\alpha w_k|^2 dx \\
& = (1 + \log(H_i/h_i))^2 \sum_{k=i,j} \left(\frac{H_k}{\eta_k}\right)^2 \frac{\bar{\alpha}_k^{\eta_k}}{\underline{\alpha}_k^{\eta_k}} |w_k|_{S_k}^2,
\end{aligned}$$

which completes the proof of (4.17) for the face terms with $\beta = 2$.

Under the additional assumption that $\alpha(x) \gtrsim \underline{\alpha}_k^{\eta_k}$ for all $x \in \Omega_k$, we can estimate (4.22) and (4.23) more directly using Lemma 4.3 and Lemma 4.5 on the whole of Ω_k instead of Ω_k, η_k , i. e.

$$(4.25) \quad \|w_k - \bar{w}_k\|_{L^2(\partial\Omega_k)}^2 \lesssim H_k |\mathcal{H}_\alpha w_k|_{H^1(\Omega_k)}^2,$$

$$(4.26) \quad \|w_k\|_{L^2(\partial\Omega_k)}^2 \lesssim H_k (1 + \log(H_k/h_k)) |\mathcal{H}_\alpha w_k|_{H^1(\Omega_k)}^2.$$

and so using (4.25) and (4.26) instead of (4.22) and (4.23) in (4.19) and (4.20) leads to the improved estimate (4.17) with $\beta = 1$.

Edge terms: For any edge $E \subset \partial\Omega_i \cap \partial\Omega_j$ Lemma 4.19 in [37] yields

$$|\psi_{ij}^E|_{H^{1/2}(\partial\Omega_i)}^2 + \frac{1}{\eta_i} \|\psi_{ij}^E\|_{L^2(\partial\Omega_i)}^2 \lesssim \sum_{k=i,j} \bar{\alpha}_k^{\eta_k} \left\{ \|w_k\|_{L^2(E)}^2 + \frac{1}{\eta_k} \|w_k\|_{L^2(\partial\Omega_k)}^2 \right\}.$$

Similar as for the face contributions, Ω_k is either floating, i. e. w_k has a vanishing average over the entire subdomain boundary $\partial\Omega_k$, or w_k vanishes at least on an edge of Ω_k . Therefore we can use Lemma 4.3 and Lemma 4.5 to obtain the bound

$$\begin{aligned}
(4.27) \quad & |\psi_{ij}^E|_{H^{1/2}(\partial\Omega_i)}^2 + \frac{1}{\eta_i} \|\psi_{ij}^E\|_{L^2(\partial\Omega_i)}^2 \\
& \lesssim \sum_{k=i,j} (1 + \log(\eta_k/h_k)) \left\{ \frac{H_k}{\eta_k} |\mathcal{H}_\alpha w_k|_{H^1(\Omega_k, \eta_k)}^2 + \left(\frac{H_k}{\eta_k}\right)^2 |\mathcal{H}_\alpha w_k|_{H^1(\Omega_k, \eta_k)}^2 \right\} \\
& \lesssim \sum_{k=i,j} (1 + \log(\eta_k/h_k)) \left(\frac{H_k}{\eta_k}\right)^2 \frac{\bar{\alpha}_k^{\eta_k}}{\underline{\alpha}_k^{\eta_k}} |w_k|_{S_k}^2.
\end{aligned}$$

Under the additional assumption $\alpha(x) \gtrsim \underline{\alpha}_i^{\eta_i}$ for all $x \in \Omega_i$, we can improve this estimate again to get linear dependency on H_k/η_k by applying the same Lemmas on Ω_i instead of Ω_i, η_i .

Vertex terms: For a vertex $V \in \partial\Omega_i \cap \partial\Omega_j$, let $\varphi_V \in V^h(\Omega_i)$ denote the nodal finite element function associated to V , i. e. $\varphi_V(V) = 1$ and $\varphi_V(x^h) = 0$ for $x^h \in \Omega_i^h \setminus \{V\}$. We have for

$k = i, j$,

$$|I^h(\theta_V w_k)|_{H^{1/2}(\partial\Omega_i)}^2 \lesssim |w_k(V) \varphi_V|_{H^1(\Omega_i)}^2 \simeq h_i |w_k(V)|^2 \lesssim \|w_k\|_{L^2(E'_k)},$$

where the edges $E'_i \in \mathcal{E}_j$ and $E'_j \in \mathcal{E}_j$ are chosen such that $V \in \overline{E'_i} \cap \overline{E'_j}$. (Note that obviously these choices are not unique.) Thus

$$|\psi_{ij}^V|_{H^{1/2}(\partial\Omega_i)}^2 + \frac{1}{\eta_i} \|\psi_{ij}^V\|_{L^2(\partial\Omega_i)}^2 \lesssim \sum_{k=i,j} \overline{\alpha}_k^{\eta_k} \left\{ \|w_k\|_{L^2(E'_k)}^2 + \frac{1}{\eta_k} \|w_k\|_{L^2(\partial\Omega_k)}^2 \right\}.$$

The result follows from the proof for the edge terms above. This completes the proof of (4.15).

4.3.2. *Estimating $P_D z_w$.* We prove that for all $w \in (\ker S)^\perp$

$$\sum_{i=1}^N |(P_D z_w)_i|^2 \lesssim \left\{ \max_{k=1}^N \left(\frac{H_k}{\eta_k} \right)^\beta \max_{j=1}^N \frac{\overline{\alpha}_j^{\eta_j}}{\underline{\alpha}_j} (1 + \log(H_j/h_j))^2 \right\} \sum_{i=1}^N |w_i|_{S_i}^2,$$

where z_w is the unique element in $\ker S$ associated with w from Lemma 3.1. Again, we restrict ourselves to the more interesting three-dimensional case. Throughout the proof we denote the (constant) components of z_w by z_i .

Note first that

$$(4.28) \quad \|B z_w\|_Q^2 = \langle B z_w, Q B z_w \rangle \simeq \sum_{\{i,j:\Gamma_{ij} \neq \emptyset\}} \min(\overline{\alpha}_i^{\eta_i}, \overline{\alpha}_j^{\eta_j}) \sum_{x^h \in \Gamma_{ij}^h} q_i(x^h) |z_i - z_j|^2.$$

Now we consider a fixed i and obtain by Lemma 4.1(ii) that

$$(4.29) \quad |(P_D z_w)_i|_{S_i}^2 \lesssim \overline{\alpha}_i^{\eta_i} \left\{ |(P_D z_w)_i|_{H^{1/2}(\partial\Omega_i)}^2 + \frac{1}{\eta_i} \|(P_D z_w)_i\|_{L^2(\partial\Omega_i)}^2 \right\}.$$

Analogously to Subsection 4.3.1, we use the characterisation (3.16) of the operator P_D , and split into face, edge and vertex terms.

Face terms: Let $F \in \mathcal{F}_i$. The contributions of F to (4.29) are given by

$$|\psi_{ij}^F|_{H^{1/2}(\partial\Omega_i)}^2 + \frac{1}{\eta_i} \|\psi_{ij}^F\|_{L^2(\partial\Omega_i)}^2 \quad \text{where} \quad \psi_{ij}^X := \min(\overline{\alpha}_i^{\eta_i}, \overline{\alpha}_j^{\eta_j})^{1/2} I^h(\theta_X(z_i - z_j)).$$

Since the components z_i of $z_w \in \ker S$ are constant, we can use Lemma 4.26 in [37] and obtain the bound

$$(4.30) \quad \begin{aligned} |\psi_{ij}^F|_{H^{1/2}(\partial\Omega_i)}^2 + \frac{1}{\eta_i} \|\psi_{ij}^F\|_{L^2(\partial\Omega_i)}^2 &\lesssim \min(\overline{\alpha}_i^{\eta_i}, \overline{\alpha}_j^{\eta_j}) \left\{ |I^h(\theta_F(z_i - z_j))|_{H^{1/2}(\partial\Omega_i)}^2 + \frac{1}{\eta_i} \|z_i - z_j\|_{L^2(F)}^2 \right\} \\ &\lesssim \min(\overline{\alpha}_i^{\eta_i}, \overline{\alpha}_j^{\eta_j}) \left\{ (1 + \log(H_i/h_i)) H_i |z_i - z_j|^2 + \frac{H_i^2}{\eta_i} |z_i - z_j|^2 \right\} \\ &\lesssim \frac{H_i}{\eta_i} \min(\overline{\alpha}_i^{\eta_i}, \overline{\alpha}_j^{\eta_j}) \underbrace{(1 + \log(H_i/h_i)) H_i}_{= \left(\frac{H_i}{h_i}\right)^2 q_i(x^h)} |z_i - z_j|^2, \end{aligned}$$

for some $x^h \in \Gamma_{ij}^h \cap F$. In the last step, we have used the special choice (3.8) for the diagonal scaling operator Q for nodes x^h that lie on a face of Ω_i . Due to our assumptions that the triangulation \mathcal{T}_i is quasi-uniform on each subdomain Ω_i and that $\text{diam } F = \mathcal{O}(H_i)$, there are

$\mathcal{O}((H_i/h_i)^2)$ nodes on F . By definition we also have $q_i(x^h) = q_i(y^h)$ for all $x^h, y^h \in \Gamma_{ij}^h \cap F$. Thus, we can rewrite (4.30) as

$$(4.31) \quad |\psi_{ij}^F|_{H^{1/2}(\partial\Omega_i)}^2 + \frac{1}{\eta_i} \|\psi_{ij}^F\|_{L^2(\partial\Omega_i)}^2 \lesssim \frac{H_i}{\eta_i} \min(\bar{\alpha}_i^{\eta_i}, \bar{\alpha}_j^{\eta_j}) \sum_{x^h \in \Gamma_{ij}^h \cap F} q_i(x^h) |z_i - z_j|^2.$$

Edge and vertex terms: Adapting the proof in [21, 37] to our case, we obtain the following bounds for the contributions of an edge $E \in \mathcal{E}_i$ and of a vertex $V \in \mathcal{V}_i$ to (4.29).

$$(4.32) \quad |\psi_{ij}^E|_{H^{1/2}(\partial\Omega_i)}^2 + \frac{1}{\eta_i} \|\psi_{ij}^E\|_{L^2(\partial\Omega_i)}^2 \lesssim \frac{H_i}{\eta_i} \min(\bar{\alpha}_i^{\eta_i}, \bar{\alpha}_j^{\eta_j}) \sum_{x^h \in \Gamma_{ij}^h \cap E} q_i(x^h) |z_i - z_j|^2,$$

$$(4.33) \quad |\psi_{ij}^V|_{H^{1/2}(\partial\Omega_i)}^2 + \frac{1}{\eta_i} \|\psi_{ij}^V\|_{L^2(\partial\Omega_i)}^2 \lesssim \frac{H_i}{\eta_i} \min(\bar{\alpha}_i^{\eta_i}, \bar{\alpha}_j^{\eta_j}) q_i(V) |z_i - z_j|^2.$$

Collecting face, edge, and vertex estimates (4.31)–(4.33) and comparing the result to (4.28) we obtain

$$(4.34) \quad |P_D z_w|_S^2 \lesssim \left(\max_{k=1}^N \frac{H_k}{\eta_k} \right) \|B z_w\|_Q^2.$$

We complete the proof by bounding $\|B z_w\|_Q^2$. First note that Lemma 3.1 implies $\|B z_w\|_Q^2 \leq \|B w\|_Q^2$, and so as in (4.28) we have

$$(4.35) \quad \|B z_w\|_Q^2 \lesssim \sum_{\{i,j:\Gamma_{ij} \neq \emptyset\}} \sum_{x^h \in \Gamma_{ij}^h} \underbrace{\min(\bar{\alpha}_i^{\eta_i}, \bar{\alpha}_j^{\eta_j}) q_i(x^h) |w_i(x^h) - w_j(x^h)|^2}_{=: r_{ij}(x^h)}.$$

We split this sum again into face, edge and vertex terms.

In (4.35) a face $F \in \mathcal{F}_i \cap \mathcal{F}_j$ contributes

$$\begin{aligned} \sum_{x^h \in \Gamma_{ij}^h \cap F} r_{ij}(x^h) &= \min(\bar{\alpha}_i^{\eta_i}, \bar{\alpha}_j^{\eta_j}) (1 + \log(H_i/h_i)) \frac{h_i^2}{H_i} \sum_{x^h \in \Gamma_{ij}^h \cap F} (w_i(x) - w_j(x))^2 \\ &\lesssim \min(\bar{\alpha}_i^{\eta_i}, \bar{\alpha}_j^{\eta_j}) (1 + \log(H_i/h_i)) \frac{1}{H_i} \|w_i - w_j\|_{L^2(F)}^2 \\ &\lesssim (1 + \log(H_i/h_i)) \left\{ \frac{\bar{\alpha}_i^{\eta_i}}{H_i} \|w_i\|_{L^2(\partial\Omega_i)}^2 + \frac{\bar{\alpha}_j^{\eta_j}}{H_j} \|w_j\|_{L^2(\partial\Omega_j)}^2 \right\}. \end{aligned}$$

Using the estimates (4.23) and (4.26) from Subsection 4.3.1, and the fact that $H_i/\eta_i \simeq H_j/\eta_j$ and $H_i/h_i \simeq H_j/h_j$ we finally obtain the bound

$$(4.36) \quad \sum_{x^h \in \Gamma_{ij}^h \cap F} r_{ij}(x^h) \lesssim (1 + \log(H_i/h_i))^2 \sum_{k=i,j} \left(\frac{H_k}{\eta_k} \right)^{\beta-1} \frac{\bar{\alpha}_k^{\eta_k}}{\underline{\alpha}_k} |w_k|_{S_k}^2,$$

where $\beta = 2$ in general and $\beta = 1$ under the additional assumption that $\alpha(x) \gtrsim \underline{\alpha}_i^{\eta_i}$ for all $x \in \Omega_i$.

Similarly, the contribution in (4.35) from an edge $E \in \mathcal{E}_i \cap \mathcal{E}_j$ can be bounded by

$$(4.37) \quad \sum_{x^h \in \Gamma_{ij}^h \cap E} r_{ij}(x^h) \lesssim \sum_{k=i,j} \bar{\alpha}_k^{\eta_k} \|w_k\|_{L^2(E)}^2 \lesssim \sum_{k=i,j} \left(\frac{H_k}{\eta_k}\right)^{\beta-1} (1 + \log(H_k/h_k)) \frac{\bar{\alpha}_k^{\eta_k}}{\underline{\alpha}_k} |w_k|_{S_k}^2,$$

where in the last step we have used Lemma 4.5 on Ω_{i,η_i} to get the estimate for $\beta = 2$, and on Ω_i to get the case $\beta = 1$, again under the additional assumption $\alpha(x) \gtrsim \underline{\alpha}_i^{\eta_i}$ for all $x \in \Omega_i$.

The contribution from a vertex $V \in \mathcal{V}_i \cap \mathcal{V}_j$ can be bounded as in Subsection 4.3.1 by

$$(4.38) \quad r_{ij}(V) = \min(\bar{\alpha}_i^{\eta_i}, \bar{\alpha}_j^{\eta_j}) h_i (w_i(V) - w_j(V))^2 \lesssim \sum_{k=i,j} \bar{\alpha}_k^{\eta_k} \|w_k\|_{L^2(E'_k)}^2$$

where E'_k are arbitrary edges in \mathcal{E}_k with $V \in \bar{E}'_k$ for $k = i, j$.

Finally, since there are a bounded number of faces, edges and vertices per subdomain, combining (4.34)–(4.38) yields the desired estimate

$$|P_D z_w|_S^2 \lesssim \max_{k=1}^N \left(\frac{H_k}{\eta_k}\right)^\beta \max_{j=1}^N \left\{ (1 + \log(H_j/h_j))^2 \frac{\bar{\alpha}_j^{\eta_j}}{\underline{\alpha}_j} \right\} \sum_{i=1}^N |w_i|_{S_i}^2.$$

which completes the proof of Lemma 3.2 for the case of three dimensions.

The above proof can easily be adapted to the case of two dimensions using in particular Part (i) instead of Part (ii) in Lemma 4.5, i. e. the discrete Sobolev-type inequalities for 2D. \square

5. NUMERICAL RESULTS

In this section we first give two examples with so-called “island” coefficients that do not vary in the vicinity of the interface, but have a jump or are even randomly distributed in the subdomain interiors. We use these examples mainly to confirm our theoretical results. In particular, we will see from the experiments that the factor H/η in our condition number bound is sharp. However, we also study more complicated multiscale and nonlinear problems where the coefficient varies also in the vicinity of the interface. We will see that our bounds are sharp in these cases as well, and that the condition number does indeed grow with $\bar{\alpha}_i^{\eta_i}/\underline{\alpha}_i^{\eta_i}$. As a remedy we present a variation to the FETI method analysed above that uses pointwise weights in Q and D_i (instead of $\bar{\alpha}_i^{\eta_i}$ on all of $\partial\Omega_i$). These are more natural and suitable for boundary layer variation and seem to lead to an extremely robust method even in the case of very high variation near the interface. We compare various weightings for the case of “edge islands” and finish the section with some nonlinear magnetic field computations.

5.1. Interior “island” coefficients. In Example 1 we choose Ω to consist of 25 squares, with an island coefficient in the centre square, cf. Figure 3, left. In that figure and in what follows H denotes the subdomain width/height and η denotes the distance of the material interface to the subdomain boundary. We set the coefficient to 1 outside the shaded square and to a constant value α_I inside. We impose Dirichlet boundary conditions on the entire boundary $\partial\Omega$ and choose a constant right hand side.

In Tables 1 and 2 we display the required numbers of PCG iterations (to achieve a relative residual reduction of 10^{-8}) and the condition numbers (estimated by the Lanczos method) for

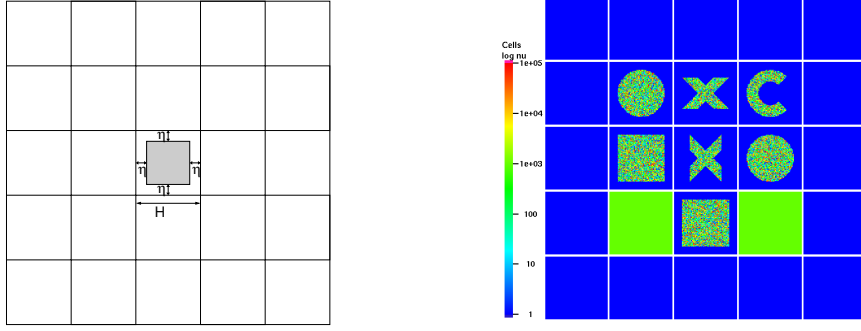


FIGURE 3. Coefficient distribution and subdomain partition in Example 1 (left) and Example 2 (right).

the case of $\alpha_I = 10^{+5}$ as well as $\alpha_I = 10^{-5}$. For comparison we have included also the cases $\alpha_I = 1$ (no jump) as well as $\eta = 0$ (jump aligned with the subdomain boundary). Finally, Figure 4 shows various estimated condition numbers when keeping $H/h = 512$ constant, but varying H/η as well as the jump, i. e. the value of α_I . From these figures we see that the linear growth in H/η is asymptotically sharp and that the case of $\alpha_I \ll 1 = \underline{\alpha}_i^{\eta_i}$ is indeed harder than $\alpha_I \gg 1$.

	$\frac{H}{h} = 4$	8	16	32	64	128	256	512
$\frac{H}{\eta} = 4$	10(10)	12(12)	14(13)	15(14)	16(15)	17(17)	18(18)	18(18)
8	–	13(12)	14(14)	15(15)	16(16)	17(17)	18(19)	18(18)
16	–	–	14(15)	15(17)	17(17)	18(19)	18(20)	18(21)
32	–	–	–	16(19)	17(19)	19(20)	19(22)	19(21)
64	–	–	–	–	19(23)	19(24)	20(25)	22(27)
128	–	–	–	–	–	24(30)	23(30)	25(31)
256	–	–	–	–	–	–	30(35)	29(36)
512	–	–	–	–	–	–	–	39(48)
$\eta = 0$	10(9)	13(11)	14(11)	15(13)	15(13)	17(15)	17(16)	18(16)
$\alpha_I \equiv 1$	10	12	13	14	15	17	18	17

TABLE 1. Example 1: Number of CG iterations; island coefficient with $\alpha_I \equiv 10^{+5}$, in brackets: $\alpha_I \equiv 10^{-5}$

	$\frac{H}{h} = 4$	8	16	32	64	128	256	512
$\frac{H}{\eta} = 4$	2.4(2.4)	3.2(3.2)	4.3(4.3)	5.4(5.5)	6.8(6.8)	8.3(8.3)	9.9(9.9)	11.7(11.7)
8	–	3.2(3.8)	4.3(5.0)	5.4(6.3)	6.8(7.9)	8.3(9.5)	9.9(11.3)	11.7(13.3)
16	–	–	4.3(8.5)	5.4(11.0)	6.8(13.4)	8.3(15.8)	9.9(18.4)	11.7(21.1)
32	–	–	–	5.5(20.7)	6.8(24.8)	8.3(29.0)	9.9(33.3)	11.7(37.8)
64	–	–	–	–	8.7(47.8)	9.4(55.6)	10.4(63.5)	11.9(71.5)
128	–	–	–	–	–	15.6(108.7)	16.0(123.8)	16.6(139.0)
256	–	–	–	–	–	–	29.6(243.8)	29.9(273.4)
512	–	–	–	–	–	–	–	57.7(540.7)
$\eta = 0$	2.4(2.4)	3.2(3.2)	4.3(4.3)	5.4(5.4)	6.8(6.8)	8.2(8.3)	9.9(9.9)	11.7(11.7)
$\alpha_I \equiv 1$	2.4	3.2	4.3	5.4	6.8	8.3	9.9	11.7

TABLE 2. Example 1: Estimated condition numbers; island coefficient with $\alpha_I \equiv 10^{+5}$, in brackets: $\alpha_I \equiv 10^{-5}$

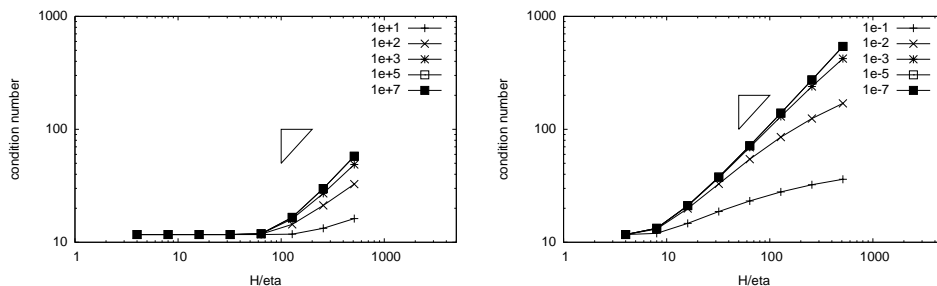


FIGURE 4. Example 1: Estimated condition numbers; $H/h = 512$, varying ratio H/η and varying magnitude of the jump α_I . Left: $\alpha_I > 1$. Right: $\alpha_I < 1$.

In Example 2, we investigate the behaviour of our method in the case of more complexly shaped island coefficients, as depicted in Figure 3, right, in order to rule out any symmetry effects. Note that here we have interface jumps (across the interface between subdomains), as well as strong variation in the subdomain interiors. The values in the interior islands are randomly distributed (piecewise constant) such that $\log_{10} \alpha = U(0, 5)$ or such that $\log_{10} \alpha = U(-5, 0)$ on each element. Again, η denotes the distance of the islands from the interface. In Tables 3 and 4 we display again the required number of PCG iterations and the estimated condition numbers. The results are similar to those for Example 1.

	$\frac{H}{h} = 8$	16	32	64	128	256	512
$\frac{H}{\eta} = 8$	15(17)	17(19)	19(21)	22(23)	24(25)	26(27)	27(28)
16	–	28(22)	20(25)	22(28)	24(30)	26(31)	28(33)
32	–	–	22(29)	24(31)	26(34)	28(37)	30(40)
64	–	–	–	27(36)	28(39)	29(41)	31(44)
128	–	–	–	–	32(43)	33(47)	35(51)
256	–	–	–	–	–	41(50)	42(56)
512	–	–	–	–	–	–	53(58)

TABLE 3. Example 2: Number of CG iterations; island coefficient with $\alpha_I \in [1, 10^{+5}]$, in brackets: $\alpha_I \in [10^{-5}, 1]$, randomly distributed.

	$\frac{H}{h} = 8$	16	32	64	128	256	512
$\frac{H}{\eta} = 8$	3.8(4.8)	4.7(6.3)	5.8(8.0)	6.9(9.8)	8.3(11.6)	9.7(13.6)	11.3(15.7)
16	–	5.8(9.9)	6.7(13.0)	7.7(15.7)	8.9(18.8)	10.3(22.0)	11.8(25.3)
32	–	–	9.6(19.5)	10.4(23.9)	11.4(29.5)	12.4(35.0)	13.7(40.3)
64	–	–	–	16.9(33.9)	17.7(43.0)	18.5(51.6)	19.4(60.1)
128	–	–	–	–	31.0(58.1)	31.8(69.5)	32.6(81.6)
256	–	–	–	–	–	58.0(86.3)	58.8(101.8)
512	–	–	–	–	–	–	107.7(122.1)

TABLE 4. Example 2: Estimated condition numbers; island coefficient with $\alpha_I \in [1, 10^{+5}]$, in brackets: $\alpha_I \in [10^{-5}, 1]$, randomly distributed.

5.2. Pointwise weights. Before we come to examples with boundary layer variation, we would like to give a recipe for a more practical choice of the weights in Q and D_i which does not require to choose a parameter η_i for each Ω_i or to compute the upper bound $\bar{\alpha}_i^{\eta_i}$ of α in

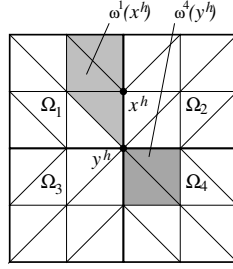


FIGURE 5. Subdomain node patches $\omega^1(x^h)$, $\omega^4(y^h)$ corresponding to the nodes x^h and y^h , cf. (5.1).

Ω_{i,η_i} . Moreover we will see below that this method is robust even if there is strong variation in the boundary layer (although a theoretical proof of this fact is unfortunately still lacking). This choice of weights is closely related to an approach by Rixen and Farhat [31, 32] called *superlumping*. In the case where the coefficients are constant on Ω_{i,η_i} (e.g. Examples 1 and 2 above) it reduces to the method described above.

Since the weights in Q and D_i are all associated with a particular node $x^h \in \Gamma^h$, it is natural to replace the values $\bar{\alpha}_i^{\eta_i}$ in the definitions of Q and D_i in (3.8) and (3.10) by meaningful point evaluations of the coefficient $\alpha(\cdot)$ at the nodes $x^h \in \Gamma^h$. We can hope that this choice leads to a more robust scheme since it incorporates the local behaviour of the coefficient along the subdomain boundaries. Let us look at a typical subdomain Ω_i . For any node $x^h \in \partial\Omega_i^h$ we define

$$(5.1) \quad \omega^i(x^h) := \bigcup \{ \bar{\tau} : \tau \in \mathcal{T}_i, x^h \in \bar{\tau} \},$$

i. e. the patch of elements in Ω_i around x^h (cf. Fig. 5). In order to get a meaningful point value of the coefficient (which is piecewise constant with respect to the elements and so in general discontinuous across element boundaries), we can choose, e.g., the following average

$$(5.2) \quad \alpha_i^{\text{mean}}(x^h) := \frac{1}{|\omega^i(x^h)|} \sum_{\tau \subset \omega^i(x^h)} |\tau| \cdot \alpha|_{\tau},$$

or the maximum

$$(5.3) \quad \alpha_i^{\text{max}}(x^h) := \max_{\tau \subset \omega^i(x^h)} \alpha|_{\tau}$$

over the patch $\omega^i(x^h)$. Using either $\hat{\alpha}_i = \alpha_i^{\text{mean}}$ or $\hat{\alpha}_i = \alpha_i^{\text{max}}$, we can define new operators \hat{Q} and \hat{D}_i by replacing the constant weights $\bar{\alpha}_i^{\eta_i}$ at the nodes $x^h \in \partial\Omega_i^h$ by $\hat{\alpha}(x^h)$: For the component $\lambda_{ij}(x^h)$ of the vector λ of Lagrange multipliers we set

$$(\hat{Q}\lambda)_{ij}(x^h) := \min [\hat{\alpha}_i(x^h), \hat{\alpha}_j(x^h)] q_i(x^h) \lambda_{ij}(x^h),$$

(cf. 3.9). \hat{D}_i is defined in the same way as D_i , but using the modified partition of unity functions

$$\hat{\delta}_j^\dagger(x^h) := \begin{cases} \hat{\alpha}_j(x^h) \left[\sum_{k \in \mathcal{N}_{x^h}} \hat{\alpha}_k(x^h) \right]^{-1} & \text{for } x^h \in \partial\Omega_j^h \cap \Gamma^h, \\ 1 & \text{for } x^h \in \partial\Omega_j^h \cap \partial\Omega^h, \\ 0 & \text{otherwise.} \end{cases}$$

Note, that this generalisation does not need any information about the boundary layers *in the algorithm* since it neither involves $\bar{\alpha}_i^{\eta_i}$ nor η_i , but only the coefficient function $\alpha(\cdot)$ itself. For $\alpha(\cdot)$ constant on the boundary layers Ω_{i,η_i} , the pointwise weights α_i^{\max} , α_i^{mean} coincide with $\bar{\alpha}_i^{\eta_i}$.

Using the coefficient distribution from Example 2 and setting $\eta = 0$, we get strong coefficient variation along the subdomain boundaries over 5 orders of magnitude. Nevertheless, using α_i^{\max} as the new weights in our method the results in Table 5 suggest that it is almost coefficient robust even in this case.

		$\frac{H}{h} = 8$	16	32	64	128	256	512
$\alpha_I \in [1, 10^{+5}]$	it	16	19	25	27	31	40	52
	cond	4.1	5.2	29.1	12.4	22.5	34.5	66.4
$\alpha_I \in [10^{-5}, 1]$	it	32	36	42	44	53	70	86
	cond	205.5	59.3	57.9	58.9	99.1	118.8	218.3

TABLE 5. Example 2: Iteration counts and estimated condition numbers; random island coefficient, $\eta = 0$.

5.3. "Edge" islands. Let us now investigate the dependency of our method(s) on coefficient variation near the interface. The coefficient distribution in Example 3 is depicted in Figure 6. As in Example 1 we have 25 subdomains with $\alpha = 1$ everywhere except for the shaded

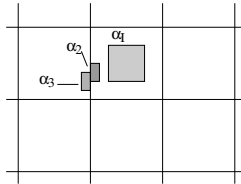


FIGURE 6. Coefficient distribution in Example 3.

regions. In the interior island we choose $\alpha_I = 10^7$. In the edge islands the coefficients are α_2 and α_3 , respectively, which we will vary in the range of $[10^{-5}, 10^{+5}]$. Table 6 displays the iteration and condition numbers for a fixed discretisation with $H/h = 64$ and for three different weightings:

- (i) First we use $\max_{x \in \Omega_i} \alpha(x)$ (denoted *max*). Here we get a very poor behaviour in the condition number (as expected).
- (ii) Then we use $\bar{\alpha}_i^{\eta_i} = \max_{x \in \Omega_{i,\eta_i}} \alpha(x)$ (denoted *layer max*), where η_i is chosen such that the value α_I disappears from the weights. This corresponds to the method described in Section 3. The behaviour in this case (albeit slightly better than for the first choice) confirms our theoretical results in Theorem 3.3, i. e. a linear growth of the condition number with $\bar{\alpha}_i^{\eta_i} / \alpha_i^{\eta_i}$ but no dependency on jumps across the subdomain interfaces. The iteration numbers do not seem to be affected as badly by the size of the coefficient variation. This is due to clustering effects in the spectrum of the preconditioned matrix, since we only introduce a very small number of islands (cf. [1, 14, 39]).
- (iii) Finally, using the pointwise weights α_i^{\max} (denoted *pw max*) defined in (5.3) results in a fully robust method with respect to any kind of variation of α_2 , α_3 , and α_I . This is very encouraging, but unfortunately we do not yet have a theoretical explanation for this robustness.

α_2	<i>max</i>		<i>layer max</i>		<i>pw max</i>		α_2	<i>max</i>		<i>layer max</i>		<i>pw max</i>	
	it	cond	it	cond	it	cond		it	cond	it	cond	it	cond
10^{-5}	61	$1.0 \cdot 10^5$	56	$2.5 \cdot 10^4$	19	6.34	10^{-5}	110	$1.0 \cdot 10^8$	25	$3.2 \cdot 10^3$	20	6.34
10^{-4}	62	$1.0 \cdot 10^4$	52	$2.5 \cdot 10^3$	20	6.34	10^{-4}	141	$1.0 \cdot 10^8$	26	$3.2 \cdot 10^2$	20	6.34
10^{-3}	56	$1.0 \cdot 10^3$	44	$2.5 \cdot 10^2$	21	6.34	10^{-3}	129	$1.0 \cdot 10^6$	27	$3.8 \cdot 10^1$	21	6.34
10^{-2}	44	$1.0 \cdot 10^2$	30	$2.6 \cdot 10^1$	21	6.34	10^{-2}	100	$1.0 \cdot 10^4$	27	$1.6 \cdot 10^1$	21	6.34
10^{-1}	29	$1.5 \cdot 10^1$	21	$6.4 \cdot 10^0$	21	6.34	10^{-1}	50	$1.0 \cdot 10^2$	26	$1.3 \cdot 10^1$	20	6.34
1	25	$1.5 \cdot 10^1$	18	$6.3 \cdot 10^0$	18	6.34	1	25	$1.5 \cdot 10^1$	18	$6.3 \cdot 10^0$	18	6.34
10^{+1}	30	$1.6 \cdot 10^1$	26	$1.3 \cdot 10^1$	21	6.37	10^{+1}	26	$1.5 \cdot 10^1$	24	$1.1 \cdot 10^1$	21	6.34
10^{+2}	47	$1.0 \cdot 10^2$	36	$2.6 \cdot 10^1$	21	6.78	10^{+2}	28	$1.5 \cdot 10^1$	27	$1.4 \cdot 10^1$	21	6.34
10^{+3}	61	$1.0 \cdot 10^3$	60	$2.5 \cdot 10^2$	21	6.88	10^{+3}	28	$3.8 \cdot 10^1$	27	$3.8 \cdot 10^1$	21	6.34
10^{+4}	76	$1.0 \cdot 10^4$	74	$2.5 \cdot 10^3$	21	6.89	10^{+4}	26	$3.2 \cdot 10^2$	27	$3.2 \cdot 10^2$	20	6.34
10^{+5}	86	$1.0 \cdot 10^5$	88	$2.5 \cdot 10^4$	21	6.89	10^{+5}	24	$3.2 \cdot 10^3$	25	$3.2 \cdot 10^3$	20	6.34

TABLE 6. Example 3 (with $H/h = 64$). Iteration numbers and estimated condition numbers for different weightings: *max* – global maximum over whole subdomain, *layer max* – maximum over boundary layer (excluding $\alpha_I = 10^{+7}$), *pw max* – pointwise weights α_i^{\max} defined in (5.3). Left: $\alpha_3 = \alpha_2$. Right: $\alpha_3 = (\alpha_2)^{-1}$.

5.4. Nonlinear magnetic field computations. In Example 4 we test two coefficient distributions coming from nonlinear magnetic field computations, similar to the ones in [23]. In the computations we use the piecewise weights α_i^{\max} in (5.3). Figure 7 displays the coefficient distribution, the subdomain partition, and the coefficient variation along one of the relevant subdomain boundaries for two cases. In both cases the global coefficient variation in the nonlinear material is approximately $7 \cdot 10^3$. However, in the first case we have a mild variation along subdomain boundaries of magnitude $\simeq 10$. In the second case the variation along the subdomain boundary is $7 \cdot 10^3$. For a fixed discretisation with $H/h = 128$ the estimated condition numbers are 8.5 and 13.7 in cases 1 and 2, respectively. The numbers of PCG iterations are 19 and 16. Since the variation in the boundary layer is mild in case 1 the good behaviour in this case is explained by our theory. The robustness in the second case is more surprising. Note also that in contrast to the usual suggestions in the literature it seems to be of benefit not to resolve the material interfaces with the subdomain partition, but rather to put the areas of largest coefficient variation into the centre of the subdomains.

ACKNOWLEDGEMENTS

Great thanks are offered to Ulrich Langer for his motivation and encouragement and to Astrid Sinwel for many fruitful discussions. The first author would like to thank the BICS Institute at the University of Bath, in particular Ivan Graham for the invitations in autumn 2006 and summer 2008. The second author would like to thank the RICAM (Austrian Academy of Sciences) at Linz for financing his stay during the special Radon semester in autumn 2007. The financial support by the Austrian Science Funds (FWF) under grant SFB F013 is gratefully acknowledged.

APPENDIX A. PROOFS OF LEMMAS 4.3 AND 4.5

For the sake of simplicity we drop the subdomain indices i and thus work on a generic regular domain Ω with boundary $\partial\Omega$ and diameter H , and with the boundary layer Ω_η of width η . Due to Definition 2.6 and Assumption A3 we can cover the discrete boundary layer

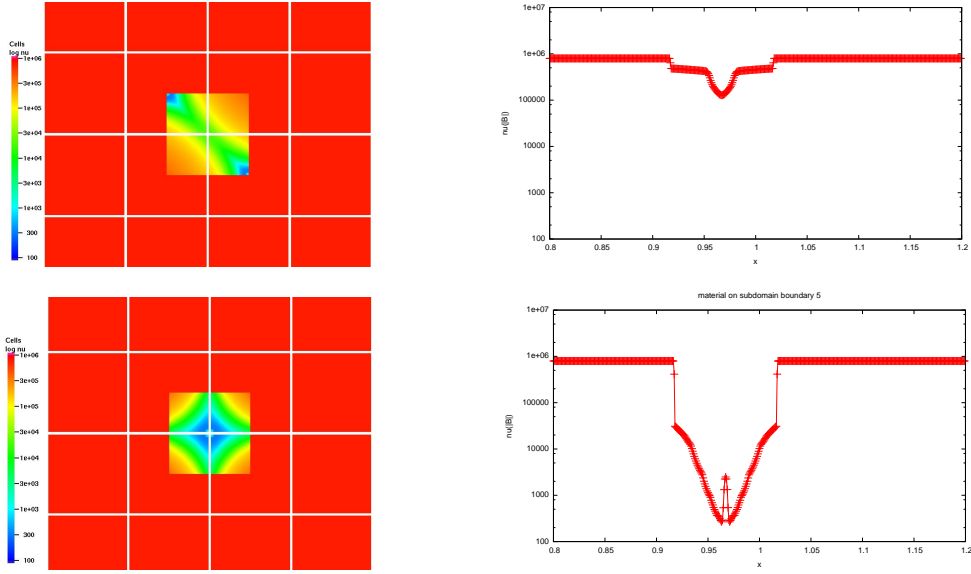


FIGURE 7. Example 4. Left: Coefficient distribution and subdomain partition. Right: Coefficient plotted along a subdomain boundary. Upper: Mild boundary layer variation. Lower: Strong boundary layer variation.

Ω_η by finitely many patches

$$(A.1) \quad \Xi_\eta := \{\omega_1, \dots, \omega_s\}.$$

The patches ω_i are regular in the sense of Definition 2.1, cf. Figure 8. They have uniform diameter η and the exterior boundary $\gamma_i := \partial\omega_i \cap \partial\Omega$ is a union of faces of ω_i with a diameter proportional to η . Due to the finite overlap assumption it is clear that there are at most $s = \mathcal{O}((H/\eta)^{d-1})$ such patches.

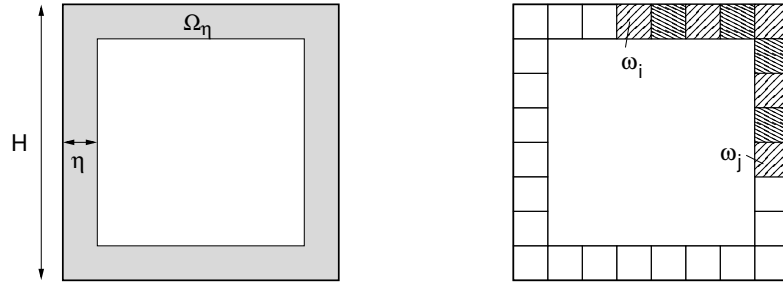


FIGURE 8. Left: Boundary layer Ω_η of diameter $\mathcal{O}(H)$ and width η . Right: Sketch of partitioning of Ω_η into patches, cf. (A.1) and the path P_{ij} connecting the patches ω_i and ω_j , cf. Definition A.1.

Definition A.1. Let $\omega_i, \omega_j \in \Xi_\eta$. We call $P_{ij} \subset \Omega_\eta$ a *path* of length M connecting the patches ω_i and ω_j , iff it is a connected union of M patches from Ξ_η such that $\omega_i, \omega_j \subset P_{ij}$.

Assumption A4. For two neighbouring patches $\omega_i, \omega_j \in \Xi_\eta$, we assume that the *compound patch* $\omega_{i,j}$ such that $\bar{\omega}_{i,j} = \bar{\omega}_i \cup \bar{\omega}_j$ is regular in the sense of Definition 2.1.

Lemma A.2. *Suppose $\Omega \subset \mathbb{R}^d$, $d = 2, 3$. Let $\omega_i, \omega_j \in \Xi_\eta$ and let P_{ij} be a path of length M connecting ω_i, ω_j .*

(i) *Then*

$$\frac{1}{\eta^d} \int_{\gamma_i} \int_{\gamma_j} |u(x) - u(y)|^2 ds_x ds_y \lesssim M |u|_{H^1(P_{ij})}^2 \quad \forall u \in H^1(\Omega_\eta).$$

(ii) *Let $d = 2$ and let $x_i \in \gamma_i$ and $x_j \in \gamma_j$ be two points on $\partial\Omega$. Then*

$$|u(x_i) - u(x_j)|^2 \lesssim M (1 + \log(\eta/h)) |u|_{H^1(P_{ij})}^2 \quad \forall u \in V^h(\Omega_\eta).$$

(iii) *Let $d = 3$ and let $e_i \subset \bar{\gamma}_i$ and $e_j \subset \bar{\gamma}_j$ be two edges on $\partial\Omega$. Then*

$$\begin{aligned} \frac{1}{\eta} \int_{e_i} \int_{e_j} |u(x) - u(y)|^2 ds_y ds_x &\lesssim M (1 + \log(\eta/h)) |u|_{H^1(P_{ij})}^2 & \forall u \in V^h(\Omega_\eta), \\ \frac{1}{\eta^2} \int_{\gamma_i} \int_{\gamma_j} |u(x) - u(y)|^2 ds_y ds_x &\lesssim M (1 + \log(\eta/h)) |u|_{H^1(P_{ij})}^2 & \forall u \in V^h(\Omega_\eta). \end{aligned}$$

Proof. Let i, j and the patch P_{ij} be fixed. Without loss of generality, we assume that the patches in Ξ_η and in the path P_{ij} are ordered in such a way that $\{\omega_k\}_{i \leq k \leq j}$ are exactly the patches in P_{ij} and $\bar{\omega}_k \cap \bar{\omega}_{k+1} \neq \emptyset$ for $i \leq k < j$. We define the average values

$$\bar{u}^k := \frac{1}{|\gamma_k|} \int_{\gamma_k} u(x) ds_x \quad \text{for } i \leq k \leq j.$$

ad (i): Let $x \in \gamma_i$ and $y \in \gamma_j$. Using the Cauchy-Schwarz inequality in \mathbb{R}^M and the fact that P_{ij} is a patch of length M we obtain

$$\begin{aligned} |u(x) - u(y)|^2 &= \left| [u(x) - \bar{u}^i] + \left[\sum_{k=i}^{j-1} \bar{u}^k - \bar{u}^{k+1} \right] + [\bar{u}^j - u(y)] \right|^2 \\ (A.2) \quad &\lesssim M \left\{ |u(x) - \bar{u}^i|^2 + \left[\sum_{k=i}^{j-1} |\bar{u}^k - \bar{u}^{k+1}|^2 \right] + |\bar{u}^j - u(y)|^2 \right\}. \end{aligned}$$

Since $|\gamma_i| \simeq |\gamma_j| \simeq \eta^{d-1}$ we can conclude that

$$\begin{aligned} \frac{1}{\eta^d} \int_{\gamma_i} \int_{\gamma_j} |u(x) - u(y)|^2 ds_x ds_y \\ \lesssim M \left\{ \frac{1}{\eta} \int_{\gamma_i} |u(x) - \bar{u}^i|^2 ds_x + \eta^{d-2} \left[\sum_{k=i}^{j-1} |\bar{u}^k - \bar{u}^{k+1}|^2 \right] + \frac{1}{\eta} \int_{\gamma_i} |\bar{u}^j - u(y)|^2 \right\}. \end{aligned}$$

Using the Poincaré inequality [37, Lemma A.18] on ω_k we obtain

$$\frac{1}{\eta} \int_{\gamma_k} |u(x) - \bar{u}^k|^2 ds_x \lesssim |u|_{H^1(\omega_k)}^2, \quad k = i, j.$$

For the terms $\eta^{d-2} |\bar{u}^k - \bar{u}^{k+1}|^2$, $k = i, \dots, j-1$, we could apply the Bramble-Hilbert lemma on the compound patches $\omega_{k,k+1}$, since the functional $u \mapsto \bar{u}^k - \bar{u}^{k+1}$ vanishes for the constant functions on $\omega_{k,k+1}$. However, the Bramble-Hilbert constant depends on the shape/size of

$\omega_{k,k+1}$. More directly, we use that $\omega_{k,k+1}$ is regular due to Assumption A4 and obtain by the Cauchy-Schwarz inequality that

$$\begin{aligned} |\bar{u}^k - \bar{u}^{k+1}|^2 &= \left(\frac{1}{|\gamma_k|} \int_{\gamma_k} u(x) - \bar{u}^{k+1} ds_x \right)^2 \\ &\lesssim \eta^{1-d} \int_{\gamma_k} |u(x) - \bar{u}^{k+1}|^2 ds_x \lesssim \eta^{1-d} \int_{\partial\omega_{k,k+1}} |u(x) - \bar{u}^{k+1}|^2 ds_x. \end{aligned}$$

On the regular domain $\omega_{k,k+1}$ we can apply the Poincaré inequality [37, Lemma A.18], using the fact that γ_k is a union of edges (resp. faces) of $\omega_{k,k+1}$ in two (resp. three) dimensions. This yields

$$\eta^{d-2} |\bar{u}^k - \bar{u}^{k+1}|^2 \lesssim \frac{1}{\eta} \|u - \bar{u}^{k+1}\|_{L^2(\partial\omega_{k,k+1})}^2 \lesssim |u|_{H^1(\omega_{k,k+1})}^2.$$

Since all the compound patches $\omega_{k,k+1}$ have only finite overlap and their union forms the path P_{ij} , we easily obtain the desired result (i).

ad (ii): Suppose $\Omega \subset \mathbb{R}^2$. Let $\tilde{\mathcal{T}}(\omega_i)$ be an auxiliary quasi-uniform mesh on ω_i of mesh width h that coincides on γ_i with the original mesh \mathcal{T} . Note that $\tilde{\mathcal{T}}(\omega_i)$ does not have to coincide with \mathcal{T} on the rest of ω_i , i. e. the patches ω_i are allowed to cut through triangles/tetrahedra in the original mesh \mathcal{T} . Let $\Pi_h^{(i)}$ denote the Scott-Zhang quasi-interpolation operator on ω_i with respect to $\tilde{\mathcal{T}}(\omega_i)$ [36]. Note that this operator is constructed such that, for each $u \in H^1(\omega_i)$, $(\Pi_h^{(i)} u)|_{\partial\omega_i} = u|_{\partial\omega_i}$ and $|\Pi_h^{(i)} u|_{H^1(\omega_i)} \lesssim |u|_{H^1(\omega_i)}$.

In (A.2) let $x = x_i \in \gamma_i$ and $y = x_j \in \gamma_j$. But now estimate the first and last term in (A.2) using Lemma 4.15 in [37] and the properties of the Scott-Zhang operator outlined above. Then

$$\begin{aligned} |u(x_i) - \bar{u}^i|^2 + |\bar{u}^j - u(x_j)|^2 &\lesssim (1 + \log(\eta/h)) \left[|\Pi_h^{(i)} u|_{H^1(\omega_i)}^2 + |\Pi_h^{(j)} u|_{H^1(\omega_j)}^2 \right] \\ &\lesssim (1 + \log(\eta/h)) \left[|u|_{H^1(\omega_i)}^2 + |u|_{H^1(\omega_j)}^2 \right]. \end{aligned}$$

The terms $|\bar{u}^k - \bar{u}^{k+1}|^2 = \eta^{d-2} |\bar{u}^k - \bar{u}^{k+1}|^2$ can be treated as before. Again because of the finite overlap assumption this immediately proves (ii).

ad (iii): Suppose $\Omega \subset \mathbb{R}^2$. Let $e_i \subset \bar{\gamma}_i$ and $e_j \subset \bar{\gamma}_j$ be two edges on $\partial\Omega$ (with $|e_i| \simeq |e_j| \simeq \eta$). It follows again from (A.2) that

$$\begin{aligned} &\frac{1}{\eta} \int_{e_i} \int_{e_j} |u(x) - u(y)|^2 ds_y ds_x \\ &\lesssim M \left\{ \int_{e_i} |u(x) - \bar{u}^i|^2 ds_x + \eta \left[\sum_{k=i}^{j-1} |\bar{u}^k - \bar{u}^{k+1}|^2 \right] + \int_{e_j} |u(x) - \bar{u}^j|^2 ds_y \right\}. \end{aligned}$$

For the first and the last term we can use Lemma 4.16 in [37]. The remaining terms are treated as in (i). This finishes the proof of the first estimate in (iii). The second estimate is shown analogously using the usual Poincaré inequality to bound the term $\int_{\gamma_i} |u(x) - \bar{u}^i|^2 ds_x$. \square

Lemma A.3. *Let $\omega_i, \omega_j \in \Xi_\eta$. There exists a path P_{ij} connecting ω_i and ω_j of length $M = \mathcal{O}(H/\eta)$.*

Proof. This follows directly from Assumption A3, i. e. from the regularity of the patches and from the finite overlap assumption. \square

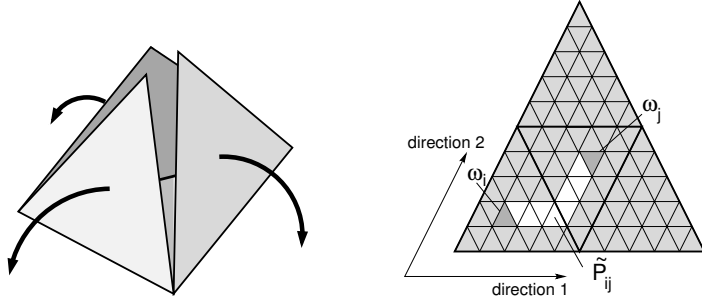


FIGURE 9. Left: Unfolding the boundary of a tetrahedron. Right: Sketch illustrating the three-dimensional path algorithm from the proof of Lemma 4.3.

Proof of Lemma 4.3 – the generalised Poincaré inequality. We start as in many direct proofs of Poincaré’s inequality from the literature: For $x, y \in \partial\Omega$, we have

$$u(x)^2 + u(y)^2 - 2u(x)u(y) = [u(x) - u(y)]^2.$$

Integrating twice over $\partial\Omega$ and using the patch decomposition from (A.1) yields

$$(A.3) \quad 2|\partial\Omega| \int_{\partial\Omega} u(x)^2 ds_x - 2 \left(\int_{\partial\Omega} u(x) ds_x \right)^2 = \int_{\partial\Omega} \int_{\partial\Omega} [u(x) - u(y)]^2 ds_x ds_y \\ \leq \sum_{i,j=1}^s \int_{\gamma_i} \int_{\gamma_j} [u(x) - u(y)]^2 ds_x ds_y.$$

Using Lemma A.2(i) we can bound each one of the double integrals on the right hand side of (A.3) from above by $\eta^d M |u|_{H^1(P_{ij})}^2$, where P_{ij} is a path of length M connecting ω_i and ω_j . Due to Lemma A.3 we know that $M \lesssim H/\eta$, and so

$$(A.4) \quad \sum_{i,j=1}^s \int_{\gamma_i} \int_{\gamma_j} [u(x) - u(y)]^2 ds_x ds_y \lesssim \eta^d \frac{H}{\eta} \sum_{i,j=1}^s |u|_{H^1(P_{ij})}^2.$$

Combining (A.3) and (A.4), and using the trivial bound $|u|_{H^1(P_{ij})}^2 \lesssim |u|_{H^1(\Omega_\eta)}^2$ as well as the fact that $s = \mathcal{O}((H/\eta)^{d-1})$ we get

$$\frac{1}{H} \|u\|_{L^2(\partial\Omega)}^2 \lesssim \left(\frac{H}{\eta}\right)^{d-1} |u|_{H^1(\Omega_\eta)}^2 + \frac{1}{H |\partial\Omega|} \left(\int_{\partial\Omega} u ds \right)^2,$$

which is the desired inequality (4.8) for $d = 2$.

In three dimensions this leads to the suboptimal quadratic factor $(H/\eta)^2$ in front of the H^1 -seminorm. In order to get the linear factor H/η in 3D we make use of an overlap argument. In the following we restrict ourselves to the case that Ω is a tetrahedron. It is straightforward to generalise the arguments to more general regular domains. We cover the boundary $\partial\Omega$ by faces of the patches ω_i and unfold and flatten the boundary, essentially as depicted in Figure 9. We introduce two main directions (cf. Figure 9) and local coordinates $i = (i_1, i_2)$ for each of the patches ω_i . We create a special path P_{ij} by starting from ω_i : first running through patches in the first direction from i_1 to j_1 keeping the second coordinate i_2 fixed, then through patches in the second direction from i_2 to j_2 keeping the first coordinate j_1 fixed, see Figure 9. We denote the two parts of P_{ij} by $P_{ij}^{(1)}$ and $P_{ij}^{(2)}$, respectively. To

improve our bound on the right hand side of (A.4) we now fix i_1 and $j = (j_1, j_2)$. Then, because of the finite overlap of the patches ω_k , we have

$$\sum_{i_2} |u|_{H^1(P_{ij}^{(1)})}^2 \lesssim |u|_{H^1(\Omega_\eta)}^2.$$

Since the remaining indices i_2 and $j = (j_1, j_2)$ can take $\mathcal{O}((H/\eta)^3)$ possible different values, we conclude that

$$\sum_{i,j=1}^s |u|_{H^1(P_{ij}^{(1)})}^2 \lesssim \left(\frac{H}{\eta}\right)^3 |u|_{H^1(\Omega_\eta)}^2.$$

Similarly, we obtain

$$\sum_{i,j=1}^s |u|_{H^1(P_{ij}^{(2)})}^2 \lesssim \left(\frac{H}{\eta}\right)^3 |u|_{H^1(\Omega_\eta)}^2.$$

Now combining this with (A.3) and (A.4) and using the fact that $P_{ij} = P_{ij}^{(1)} \cup P_{ij}^{(2)}$, we get (4.8) for $d = 3$.

If the mean value $1/|\partial\Omega| \int_{\partial\Omega} u(x) ds_x$ is replaced by an edge or face in two or three dimensions (resp.), the above proof can be easily modified by integrating twice over the edge or over the face (resp.) in (A.3) instead of integrating twice over $\partial\Omega$. \square

Proof of Lemma 4.5 – the generalised discrete Sobolev-type inequality. (i) Let $d = 2$ and let $\zeta(u)$ be a point evaluation at a point $x_i \in \partial\Omega$. Then $x_i \in \partial\omega_i$ for some patch ω_i . Since $u \in V^h(\Omega_{i,\eta_i}) \subset \mathcal{C}(\bar{\Omega}_{i,\eta_i})$ we can also find another distinguished patch $\omega_j \in \Xi_\eta$ and a point $x_j \in \bar{\omega}_j$ where the L^∞ -norm of $u - \zeta(u)$ is attained. Thus it follows from Lemma A.2(ii) that

$$\|u - \zeta(u)\|_{L^\infty(\partial\Omega)}^2 = |u(x_j) - u(x_i)|^2 \lesssim \frac{H}{\eta} (1 + \log(\eta/h)) |u|_{H^1(P_{ij})}^2.$$

Since the path P_{ij} is a subset of Ω_η this completes the proof of (4.10) for case (a), i. e. point evaluations. However, thanks to the continuity of u we can also find a distinguished point $x_i \in \partial\Omega$ such that $\zeta(u) = u(x_i)$ in the remaining two cases (b) and (c), and so the proof of those case follows immediately. The proof of the L^2 bound is also immediate from (4.10).

(ii) In three dimensions, we restrict ourselves to the proof of (4.12) in the case of face averages, i. e. we prove

$$\|u - \zeta(u)\|_{L^2(E)}^2 \lesssim \frac{H}{\eta} (1 + \log(\eta/h)) |u|_{H^1(\Omega_\eta)}^2,$$

for the case that $\zeta(u) = \frac{1}{|F|} \int_F u(x) ds_x$, where F is a face of $\partial\Omega$ and E is an edge of $\partial\Omega$. The proofs of the remaining cases are similar.

Firstly, we can cover the edge E by N_E edges e_1, \dots, e_{N_E} of the patches $\{\omega_j\}$, where $N_E \lesssim H/\eta$. Similarly, the face F can be covered by N_F sets $\gamma_1, \dots, \gamma_{N_F}$ where $\gamma_j := \partial\omega_j \cap \partial\Omega$

as before and $N_F \lesssim (H/\eta)^2$. Hence, using Lemma A.2(iii) we obtain

$$\begin{aligned} \|u - \zeta(u)\|_{L^2(E)}^2 &= \int_E \left| u(x) - \frac{1}{|F|} \int_F u(y) \right|^2 ds_y ds_x = \int_E \left| \frac{1}{|F|} \int_F u(x) - u(y) ds_y \right|^2 ds_x \\ &\leq \frac{1}{|F|} \int_E \int_F |u(x) - u(y)|^2 ds_y ds_x \leq \frac{1}{|F|} \sum_{i=1}^{N_E} \sum_{j=1}^{N_F} \int_{e_i} \int_{\gamma_j} |u(x) - u(y)|^2 ds_y ds_x \\ &\lesssim \frac{1}{|F|} \sum_{i=1}^{N_E} \sum_{j=1}^{N_F} M_{ij} (1 + \log(\eta/h)) |u|_{H^1(P_{ij})}^2, \end{aligned}$$

where the path P_{ij} of length $M_{ij} \lesssim H/\eta$ is chosen as in the proof of Lemma 4.3. Now using the same argumentation as in that proof we obtain the desired estimate. \square

REFERENCES

- [1] B. Aksoylu, I. G. Graham, H. Klie, and R. Scheichl. Towards a rigorously justified algebraic preconditioner for high-contrast diffusion problems. *Comput. Visual. Sci.*, 2008. DOI 10.1007/s00791-008-0105-1.
- [2] R. E. Alcouffe, A. Brandt, J. J. E. Dendy, and J. W. Painter. The multi-grid method for the diffusion equation with strongly discontinuous coefficients. *SIAM J. Sci. Comput.*, 2(4):430–454, 1981.
- [3] J. H. Bramble, J. E. Pasciak, and A. H. Schatz. The construction of preconditioners for elliptic problems by substructuring, IV. *Math. Comp.*, 53(187):1–24, 1989.
- [4] S. C. Brenner. Analysis of two-dimensional FETI-DP preconditioners by the standard additive Schwarz framework. *Electron. Trans. Numer. Anal.*, 16:165–185, 2003.
- [5] S. C. Brenner and Q. He. Lower bounds for three-dimensional nonoverlapping domain decomposition algorithms. *Numer. Math.*, 93(3):445–470, 2003.
- [6] T. F. Chan and T. Mathew. Domain decomposition methods. In *Acta Numerica 1994*. Cambridge University Press, 1994.
- [7] K. A. Cliffe, I. G. Graham, R. Scheichl, and L. Stals. Parallel computation of flow in heterogeneous media modelled by mixed finite elements. *J. Comput. Phys.*, 164(2):258–282, 2000.
- [8] C. R. Dohrmann. A preconditioner for substructuring based on constrained energy minimization. *SIAM J. Sci. Comput.*, 25(1):246–258, 2003.
- [9] C. R. Dohrmann, A. Klawonn, and O. B. Widlund. Domain decomposition for less regular subdomains: Overlapping Schwarz in two dimensions. *SIAM J. Numer. Anal.*, 46(4):2153–2168, 2008.
- [10] Z. Dostál, D. Horák, and R. Kučera. Total FETI – An easier implementable variant of the FETI method for numerical solution of elliptic PDE. *Commun. Numer. Methods Eng.*, 22(12):1155–1162, 2006.
- [11] L. C. Evans. *Partial Differential Equations*, volume 19 of *Graduate Studies in Mathematics*. American Mathematical Society, Providence, RI, 1998.
- [12] C. Farhat, M. Lesoinne, P. Le Tallec, K. Pierson, and D. Rixen. FETI-DP: A dual-primal unified FETI method I: A faster alternative to the two-level FETI method. *Internat. J. Numer. Methods Engrg.*, 50:1523–1544, 2001.
- [13] C. Farhat and F.-X. Roux. A method of finite element tearing and interconnecting and its parallel solution algorithm. *Int. J. Numer. Meth. Engrg.*, 32:1205–1227, 1991.
- [14] I. G. Graham and M. J. Hagger. Unstructured additive Schwarz-conjugate gradient method for elliptic problems with highly discontinuous coefficients. *SIAM J. Sci. Comput.*, 20(6):2041–2066, 1999.
- [15] I. G. Graham, P. O. Lechner, and R. Scheichl. Domain decomposition for multiscale PDEs. *Numer. Math.*, 106(4):589–626, 2007.
- [16] I. G. Graham and R. Scheichl. Robust domain decomposition algorithms for multiscale PDEs. *Numerical Methods for Partial Differential Equations*, 23:859–878, 2007.
- [17] I. G. Graham and R. Scheichl. Coefficient-explicit condition number bounds for overlapping additive Schwarz. In U. Langer, M. Discacciati, D. E. Keyes, O. B. Widlund, and W. Zulehner, editors, *Domain Decomposition Methods in Science and Engineering XVII*, volume 60 of *Lecture Notes in Computational Science and Engineering*, pages 365–372, Berlin Heidelberg, 2008. Springer.
- [18] A. Klawonn and O. Rheinbach. Inexact FETI-DP methods. *Inter. J. Numer. Methods Engrg.*, 69:284–307, 2007.

- [19] A. Klawonn and O. Rheinbach. Robust FETI-DP methods for heterogeneous three dimensional elasticity problems. *Comput. Methods Appl. Mech. Engrg.*, 196:1400–1414, 2007.
- [20] A. Klawonn, O. Rheinbach, and O. B. Widlund. An analysis of a FETI-DP algorithm on irregular subdomains in the plane. Technical report TR2007–889, Courant Institute, New York, 2007.
- [21] A. Klawonn and O. B. Widlund. FETI and Neumann-Neumann iterative substructuring methods: connections and new results. *Comm. Pure Appl. Math.*, 54(1):57–90, 2001.
- [22] A. Klawonn, O. B. Widlund, and M. Dryja. Dual-primal FETI methods for three-dimensional elliptic problems with heterogeneous coefficients. *SIAM J. Numer. Anal.*, 40(1):159–179, 2002.
- [23] U. Langer and C. Pechstein. Coupled finite and boundary element tearing and interconnecting solvers for nonlinear potential problems. *ZAMM Z. Angew. Math. Mech.*, 86(12), 2006.
- [24] J. Mandel and C. R. Dohrmann. Convergence of a balancing domain decomposition by constraints and energy minimization. *Numer. Lin. Alg. Appl.*, 10:639–659, 2003.
- [25] J. Mandel, C. R. Dohrmann, and R. Tezaur. An algebraic theory for primal and dual substructuring methods by constraints. *Appl. Numer. Math.*, 54:167–193, 2005.
- [26] J. Mandel and R. Tezaur. Convergence of a substructuring method with Lagrange multipliers. *Numer. Math.*, 73:473–487, 1996.
- [27] J. Mandel and R. Tezaur. On the convergence of a dual-primal substructuring method. *Numer. Math.*, 88:543–558, 2001.
- [28] G. Of. The all-floating BETI method: Numerical results. In U. Langer, M. Discacciati, D. E. Keyes, O. B. Widlund, and W. Zulehner, editors, *Domain Decomposition Methods in Science and Engineering XVII*, volume 60 of *Lecture Notes in Computational Science and Engineering*, pages 295–302, Berlin Heidelberg, 2008. Springer.
- [29] C. Pechstein. Analysis of dual and dual-primal tearing and interconnecting methods in unbounded domains. SFB-Report 2007-15, SFB “Numerical and Symbolic Scientific Computing” F013, Johannes Kepler University of Linz, August 2007. http://www.sfb013.uni-linz.ac.at/~sfb/reports/2007/pdf-files/rep_07-15_pechstein.pdf.
- [30] C. Pechstein. Boundary element tearing and interconnecting methods in unbounded domains. *Appl. Num. Math.*, 2008. accepted for publication.
- [31] D. Rixen and C. Farhat. Preconditioning the FETI method for problems with intra- and inter-subdomain coefficient jumps. In P. E. Bjørstad, M. Espedal, and D. Keyes, editors, *Ninth International Conference on Domain Decomposition Methods*, pages 472–479, 1997. <http://www.ddm.org/DD9/Rixen.pdf>.
- [32] D. Rixen and C. Farhat. A simple and efficient extension of a class of substructure based preconditioners to heterogeneous structural mechanics problems. *Internat. J. Numer. Methods Engrg.*, 44:489–516, 1999.
- [33] J. Ruge and K. Stüben. Efficient solution of finite difference and finite element equations by algebraic multigrid (AMG). In D. J. Paddon and H. Holstein, editors, *Multigrid Methods for Integral and Differential Equations*, IMA Conference Series, pages 169–212, Oxford, 1985. Clarendon Press.
- [34] M. Sarkis. Nonstandard coarse spaces and Schwarz methods for elliptic problems with discontinuous coefficients using non-conforming elements. *Numer. Math.*, 77(3):383–406, 1997.
- [35] R. Scheichl and E. Vainikko. Additive Schwarz and aggregation-based coarsening for elliptic problems with highly variable coefficients. *Computing*, 80(4):319–343, 2007.
- [36] L. R. Scott and S. Zhang. Finite element interpolation of non-smooth functions satisfying boundary conditions. *Math. Comp.*, 54:483–493, 1990.
- [37] A. Toselli and O. Widlund. *Domain Decomposition Methods – Algorithms and Theory*, volume 34 of *Springer Series in Computational Mathematics*. Springer, Berlin, Heidelberg, 2005.
- [38] P. Vanek, J. Mandel, and M. Brezina. Algebraic multigrid by smoothed aggregation for 2nd and 4th order elliptic problems. *Computing*, 56(3):179–196, 1996.
- [39] J. Xu and Y. Zhu. Uniform convergent multigrid methods for elliptic problems with strongly discontinuous coefficients. Technical Report AM311, Department of Mathematics, Penn State, Pennsylvania, USA, 2007. to appear in *Math. Mod. Meth. Appl. Sci.*
- [40] W. Zheng and H. Qi. On Friedrichs–Poincaré-type inequalities. *J. Math. Anal. Appl.*, 304:542–551, 2005.